Ji et al. Journal of Nanobiotechnology (2025) 23:354
https://doi.org/10.1186/s12951-025-03437-4

Journal of Nanobiotechnology

RESEARCH Open Access

M2-ApoBDs as a therapeutic strategy for systemic lupus erythematosus: targeted macrophage reprogramming and treg differentiation

Juan Ji[1†], Shaoying Yang[2†], Yongxin Xu[1†], Qian He[1], Qian Liang[3], Guijuan Feng[4], Yunfei Xia[1], Mei Yang[3], Yuting Huang[3], Junling Yang[3], Chen Dong[3], Rui Zhao[3], Yunan Wang[1], Genkai Guo[1], Xiaoqi Sha[1], Jing Li[1], Yuehua Guo[3*] and Zhifeng Gu[1,3*]

Abstract

Systemic lupus erythematosus (SLE) is a chronic autoimmune disorder that affects various organs and systems, significantly impacting patients' health and quality of life. Conventional drugs, including glucocorticoids and standard immunosuppressive drugs, may not be enough to achieve a satisfactory therapeutic outcome in some refractory SLE patients. The abnormal phenotype and function of macrophages participate in the development of SLE. The targeted delivery to reprogram macrophage in SLE has been a long-standing challenge. Apoptotic bodies (ApoBDs) are essential for intercellular communications. This study aims to explore an effective and targeted treatment to SLE via macrophage reprogramming and Treg differentiation. In this work, we found that M2 macrophages-derived ApoBDs (M2-ApoBDs) could selectively target and localize to the spleen, where they were engulfed by splenic macrophages (phagocytic rate 73.4%). Single-cell RNA sequencing revealed that the efferocytosis of M2-ApoBDs triggered transcriptional changes in M2 (anti-inflammatory) macrophages within the spleen, subsequently promoting the differentiation of Treg cells in vivo. Immunological experiments revealed that M2-ApoBDs prompted the reprogramming of M2 macrophages in vitro, which subsequently influenced Treg cell differentiation via ligand-receptor interactions. In SLE mice, M2-ApoBDs alleviated the disease progression, including 24-hours urinary protein, plasma creatinine, plasma C3 levels, and glomerular sclerosis and interstitial fibrosis. These findings show that M2-ApoBDs can targeted-modulate macrophage polarization and Treg immune regulation, offering a novel therapeutic strategy for the effective treatment of SLE.

[†]Juan Ji, Shaoying Yang and Yongxin Xu contributed equally to this work.

*Correspondence:
Yuehua Guo
guoyuehuanju@163.com
Zhifeng Gu
guzf@ntu.edu.cn

Full list of author information is available at the end of the article

Keywords Systemic lupus erythematosus, Apoptotic bodies, Macrophages reprogramming, Targeted therapy, Immune regulation

Graphical Abstract

Schematic diagram of the findings of this study. (**A**) Scheme of M2 Mφ and derived-ApoBDs preparation. (**B**)The transplantation of ApoBDs. (**C**) Immune regulation of M2-ApoBDs. (**D**) Illustration of M2-ApoBDs therapy in SLE model.

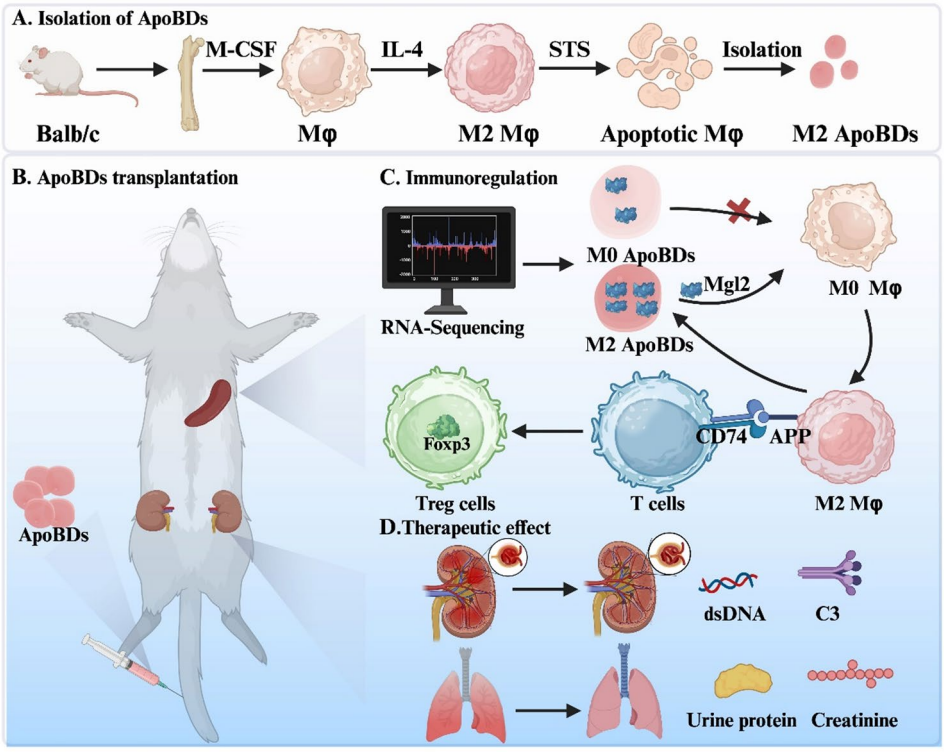

Introduction

Systemic lupus erythematosus (SLE) is a chronic and severe autoimmune disease that can affect virtually any organ system, including the lungs, kidneys, and hematologic system, among others. It predominantly occurs in young women [1]. Current therapeutic strategies for SLE involve corticosteroids, antimalarial drugs, and immunosuppressants, which are not always effective and may cause some severe side effects. A subset of patients fails to respond to existing therapies, and are at high risk for organ failure and even death. Young women, who make up the majority of those affected, continue to face the threat of early mortality [2]. Consequently, there is an urgent need for safe, effective, and innovative therapies for SLE.

Accumulated studies have suggested that both the innate and adaptive immune responses are crucial in the pathogenesis of SLE [3]. Macrophages, key effectors and regulators in the innate immune system, can perform phagocytosis, release pro-inflammatory factors, and present antigens to T cells [4]. These macrophages exhibit plasticity, differentiating into either pro-inflammatory M1 or anti-inflammatory M2 phenotypes in response to specific immune microenvironmental cues [5]. Previous research has suggested that imbalance of M1/M2 macrophages polarization affects the development of SLE. Lupus flares are linked to a relative rise in the frequency of M1/M2 macrophages [6]. Identifying potential targets for macrophage polarization, thus increasing the proportion of M2 macrophages, can offer insights into new biological treatment strategies for SLE [7]. Previous study showed that adoptive transplantation of M2 macrophages, but not M1 macrophages, significantly improved SLE clinical manifestation in clodronate

(to eliminate macrophages)- and ALD-DNA-treated mice [8]. Therefore, increasing the proportion of M2 macrophages is expected to be the one of the important means of SLE treatment. However, systemic administration of intact M2 macrophages faces numerous possible challenges. For instance, the functionality and/or effectiveness of M2 macrophages can be influenced by storage and transportation conditions, and the characteristics of transplanted M2 macrophages might revert to M1 macrophages because of oxidative stress and inflammatory environments in vivo [9, 10]. Transplanted living immune cells are prone to death in vivo due to hypoxia, inflammation or immune clearance, leading to unstable therapeutic effects. The current cell therapies rely on paracrine effects of living cells, but the release profiles of cytokines are difficult to precisely control, which may lead to cytokine storm. Therefore, there is a need for more stable, convenient, and safe treatments.

Extracellular vesicles (EVs), including exosomes, microvesicles, and apoptotic bodies (ApoBDs), are membrane-bound structures originating from cells and carry various bioactive molecules, such as proteins, lipids, mRNAs, microRNAs, and DNA [11–13]. Our previous study showed that exosomes from bone marrow-mesenchymal stem cells exerted beneficial therapeutic effects on osteoarthritis [14]. Wang et al. reported that peritoneal M2 macrophage-derived EVs, taken up by macrophages, inhibited multiple key proinflammatory pathways and attenuated infectious disease-related cytokine storms [15]. ApoBDs are a subset of EVs. Like microvesicles and exosomes, ApoBDs exert therapeutic effects by modulating diverse recipient cell populations, encompassing both professional phagocytes and adjacent non-professional cells [16]. Unlike exosomes and microvesicles, ApoBDs are formed during the late stages of apoptosis when chromatin and the nucleus condense, encapsulating intact organelles, nucleosome fragments, and chromatin debris, exhibiting more abundant and intact cargo contents [17]. Phagocytes (e.g. macrophages) could recognize 'find-me' signals expressed by ApoBDs and 'eat-me' signals on the ApoBDs to engulf them. Therefore, ApoBDs can be engulfed more readily by macrophages than other EVs. The homing ability of exosomes and MVs depend on passive diffusion mechanisms, but target cells of ApoBDs are less variable, markedly improving targeting efficiency [18]. ApoBDs exhibit natural immunoregulatory potential through their intrinsic phagocyte-targeting specificity, which facilitates precise modulation of inflammatory responses [19]. Based on the potential of ApoBDs to unleash powerful biological functions, ApoBDs have emerged as new therapeutic opportunities in SLE.

In this study, we isolated and characterized M2 macrophages and derived-ApoBDs successfully. We further demonstrated that most of ApoBDs were captured by spleen tissue, especially spleen macrophages, which provided a possibility to regulate the polarization of macrophages. Results showed that efferocytosis of M2-ApoBDs could induce transcriptional reprogramming of spleen macrophages and then modulated Treg cells differentiation, based on single-cell RNA sequencing in vivo. M2-ApoBDs induced M2 macrophages reprogramming in vitro, then induced M2 macrophage modulated the differentiation of Treg cells through this ligand–receptor interaction. At last, the therapeutic effect of M2-ApoBDs on treating SLE was investigated. We found that systemic administration of M2-ApoBDs could alleviate the development of SLE by macrophage reprogramming and Treg differentiation. Taken together, M2-ApoBDs represents a promising strategy for SLE therapy.

Materials and methods

Mice and treatments

10-week-old female MRL/lpr mice, MRL/mpj mice and BALB/c mice were sourced from Shanghai SLAC Laboratory Animal Institute Co. Ltd. MRL/lpr mice ($n = 15$) and MRL/mpj mice ($n = 5$) were housed in a pathogen-free environment at the Experimental Animal Center of Nantong University. The Ethics Committee of Nantong University granted approval for All animal procedures (No. S20230818-002). The mice were intravenously administrated with ApoBDs (appropriately 100 μg on the basis of protein measurement) or vehicle control (PBS) once a week for 8 weeks.

Isolation, culture and identification of BMDMs

BMDMs were generated by extracting bone marrow cells from tibias and femurs of BALB/c mice. Freshly extracted cells were cultured in high-glucose DMEM (Servicebio, China) with the addition of 10% fetal bovine serum (FBS) (Gibco, USA), 1% penicillin/streptomycin (NCM Biotech, China) and 20 ng/mL recombinant mouse macrophage colony-stimulating factor (M-CSF) (PeproTech, USA). Following a 7-day induction period, mature BMDMs were collected and characterized by flow cytometry with percp/cy5.5-conjugated anti-F4/80 (BioLegend, USA). Mature BMDMs were utilized for subsequent assays. BMDMs were induced to M2 Mϕ by incubating with 50 ng/mL recombinant mouse IL-4 (PeproTech, USA) proteins for 48 h. The M2 Mϕ were then harvested and analyzed using flow cytometry with percp/cy5.5-conjugated anti-F4/80, and PE-conjugated CD206 (BioLegend, USA).

Induction of BMDMs apoptosis

BMDMs were rinsed two times with PBS, and the culture medium was replaced with a complete medium that included EV-depleted FBS (SBI, USA) and 250 nM staurosporine (STS) (Beyotime, China). After 12 h treatment, apoptosis in BMDMs was assessed using the Annexin

V-FITC/PI Apoptosis Detection Kit (Vazyme, China) as per the provided guidelines.

Collection, isolation and identification of BMDM-ApoBDs

Following the initiation of apoptosis, a series of centrifugation steps were performed to isolate ApoBDs. In particular, the media were taken from the petri dish and centrifuged at 300 × g for 10 min to remove cellular debris. Subsequently, the leftover supernatant was centrifuged at 3000 × g for 30 min to collect the ApoBDs.

For transmission electron microscope (TEM) observation, ApoBDs were preserved with 2% paraformaldehyde and placed on a formvar-coated grid. Then, ApoBDs were negatively stained using 2% uranyl acetate. Stained ApoBDs were washed with double-steamed water. After drying at room temperature, images were captured. The particle size distribution of ApoBDs was measured by nanoparticle tracking analysis (NTA).

To detect apoptotic markers, isolated ApoBDs were analyzed through western blotting with anti-Caspase-3 antibodies (Proteintech, China). Additionally, ApoBDs were marked using Annexin-V-FITC labeling reagent (Vazyme, China), then examined with a confocal microscope and analyzed via flow cytometry.

Bioluminescence imaging in vivo

For studying the bio-distribution of ApoBDs through whole-body imaging, 100 μg of ApoBDs in 100 μL were tagged with DiR near-infrared fluorescent dye and subsequently administered to mice through the tail vein. The IVIS Lumina XRMS system was used to perform in vivo fluorescence imaging on anesthetized mice at 2 h, 6 h, 12 h and 24 h post-injection. Following in vivo imaging, the mice were euthanized, and their organs were extracted for ex vivo imaging. The fluorescence intensity was measured using the Living Image software.

ApoBDs uptake by spleen macrophages in vivo

To confirm the uptake of ApoBDs in spleen tissue, purified ApoBDs were tagged with Dil (Beyotime, China) following the manufacturer's guidelines and administered intravenously to mice. At 24 h after injection, spleen was harvested to conduct the subsequent experiments. To further observe how macrophages take up ApoBDs in vivo, we employed flow cytometry and immunofluorescence staining techniques. On the one hand, the suspension of single-cells was prepared from the spleen tissues. Then, splenocytes were unfrozen, resuspended with FACS buffer, washed and centrifuged (700 g for 5 min at 4 °C) twice and resuspended with PBS and FBS. Each sample was incubated for 30 min in darkness at ambient temperature using a range of anti-mouse monoclonal antibodies (BD or Biosciences), including B220-APC, CD3-APC-cy7, CD4-FITC, CD8-AF700, CD19-BV510, and F4/80-percp-cy5.5. The samples were examined using a BD Fortessa FACS Calibur (USA) and analyzed with FlowJo software. On the other hand, the spleen was preserved in 4% paraformaldehyde, cryoprotected with 30% sucrose, and encased in optimal cutting temperature (OCT) medium. Subsequently, 4 μm cryosections were created using a Leica instrument from Germany, and immunofluorescent staining was conducted on spleen sections to detect the macrophage marker F4/80. Then, spleen cryosections were incubated with DAPI (Abcam, UK) for nuclear staining. Images captured with a Zeiss microscope were analyzed through the ImageJ software.

ApoBDs uptake by BMDMs in vitro

In order to observe the uptake of ApoBDs by BMDMs in vitro, ApoBDs were labeled with Dil (Beyotime, China) according to the provided guidelines. ApoBDs were separated through centrifugation and rinsed twice with PBS to remove any remaining unbound Dil dye. To investigate ApoBDs uptake using fluorescence microscopy, BMDMs were placed in 24-well chamber slides with high-glucose DMEM containing 10% EV-depleted FBS for 24 h and then incubated with the ApoBDs. The cells were subsequently fixed with 4% paraformaldehyde (Beyotime, China) for 15 min, blocked at room temperature for 30 min, stained with DAPI (Abcam, UK) for nuclei staining, and finally observed under a Zeiss microscope.

Western blot analysis

Cells or ApoBDs samples were broken down in radioimmunoprecipitation assay (RIPA) buffer (Beyotime, China) with added protease inhibitor (Beyotime, China). The total protein concentration was determined using Nanodrop 2000 (Thermofisher, USA). Proteins in equal quantities were separated using 10% sodium dodecyl sulfate-polyacrylamide gels (SDS-PAGE) and subsequently transferred onto polyvinylidene difluoride (PVDF) membranes (Millipore, USA). PVDF membrane was treated with a 5% skim milk solution for blocking, followed by an overnight incubation at 4℃ with one of the primary antibodies: anti-CD206, anti-CD86, or anti-iNOS (Proteintech, China). The PVDF membranes were treated with HRP- conjugated secondary antibodies at room temperature for two hours. Protein bands on the membranes were detected with an enhanced chemiluminescence kit from NCM Biotech, China, and their intensity was measured using ImageJ software.

RNA isolation and qRT-PCR

Samples of BMDMs were collected and rinsed with PBS. Total RNA was extracted using the Bioteke RNA Isolation Kit (Bioteke Corporation, Beijing, China) according to the manufacturer's recommended protocol. Following the manufacturer's instructions, the mRNA

was converted into cDNA with the RevertAid First Strand cDNA Synthesis Kit (Thermo Fisher, USA). The QuantStudio™ 5 real-time PCR detection system, using SYBR Green PCR mix from Vazyme Biotech in China, was utilized to conduct real-time polymerase chain reaction (PCR). The primers used were designed by RiboBio (China). The variations in mRNA levels were determined using the delta-delta Ct technique, with GAPDH serving as the reference gene.

RNA sequencing (RNA-seq) analysis

According to the manufacturer's guidelines, Trizol (Invitrogen, USA) was used to extract total RNA from apoptotic BMDMs and derived ApoBDs. RNA sequencing libraries, with insert sizes between 100 and 500 base pairs, were created and sequenced on the Illumina NovaSeq 6000 PE150 platform at Wuhan Biobank in China. A small number of Reads in Raw Data obtained by high-throughput sequencing include sequencing connectors, low-quality bases, etc. In order to ensure the quality of information analysis, Fastq was used in this project to conduct quality control on Raw Data and Clean Data was obtained [20]. Subsequent analyses utilized this Clean Data. The R programming language was utilized for data processing and analysis. For normalizing counts and analyzing differential gene expression in RNA-seq data, the DESeq2 1.4.5 R package was utilized. Differentially expressed genes (DEGs) (Fold change > 1.5 and $p < 0.05$) were selected for subsequent functional analysis using GO and KEGG databases.

Cell suspensions Preparation and quality control of single cell RNA-sequencing (scRNA-seq)

Spleen tissues were freshly harvested from mice, rinsed with ice-cold PBS, and then processed to create single-cell suspensions. Prior to creating single cell suspensions, the fresh spleen tissues were divided into two sections: one for assessing immune regulation via flow cytometry analysis and the other for preparing single cell suspensions for scRNA-seq. To create cDNA libraries, the suspensions were incorporated into gel bead emulsions using the GemCode Single-Cell platform (10X Genomics) and subsequently sequenced on a Hiseq 2500/4000 system (Illumina) at Gene Denovo Biotechnology in Guangzhou, China. The counts quantification, genome alignment and data quality control were performed through 10X Genomics Cell Ranger software (version 3.1.0). In summary, a matrix of raw unique molecular identifier (UMI) counts was created, and reads with poor-quality barcodes and UMIs were excluded. For UMI counting, reads that were uniquely aligned to the transcriptome and overlapped an exon by at least 50% were taken into account. Following quality assessment, gene expressions were standardized using LogNormalize, a method for global scaling normalization. Afterward, we utilized a technique called Harmony to combine all the samples, thereby reducing any possible batch effects. Subsequently, principal component analysis was performed on the combined expression matrix to reduce dimensions.

Cell clustering and annotation

Cells were clustered by using Seurat [21]. In brief, the cells were embedded in a shared-nearest neighbor graph and partitioned into highly interconnected quasi-populations based on the calculated distances between cells of the principal components. Subsequently, the Louvain method was employed to cluster and group the cells, and the results were visualized using UMAP plots. The log-normalized matrices were loaded onto Single R programs to annotate the cell kinds. The cells were then classified by comparing their gene expression from scRNA-seq with reference cell types. After that, as previously documented, the annotation was manually adjusted using the conventional markers [22].

Pathway analysis

The analysis of pathways was conducted to identify key pathways and cellular processes enriched in various cell groups. To identify differentially expressed genes in cell subsets, the gene expression in a specific cluster was compared to the rest of the cells using the Wilcoxon rank-sum test, applying a fold change greater than 2 and an adjusted p-value less than 0.05 as thresholds. Subsequently, the genes with differential expression underwent pathway analysis, which encompassed GO enrichment and KEGG analysis. Additionally, the GSEA for the specified cell subsets was performed using the desktop application available at http://software.broadinstitute.org/gsea/index.jsp.

Prediction of cellular crosstalk

Cellchat was used to predict relationships between different cell types based on the quantity of surface ligand-receptor interactions. Analysis was only done when the relevant ligands or receptors were expressed by more than 10% of the examined cells in that specific cell cluster. After that, the enhanced ligand-receptor from the previous study was used to evaluate the interaction relationship and network diagram between the cells. Furthermore, the ligand-target gene regulatory potential analysis and ligand activity prediction were carried out using NicheNet. Spearman's correlation analysis was carried out to evaluate the proportions of gene expression association of pairwise cell type, and$|Rs| > 0.6$ and FDR < 0.05 was considered as significant correlation.

Pseudotime trajectory analysis

Monocle2 was utilized to conduct pseudotime trajectory analysis, aiming to forecast and chart the differentiation of Treg subsets in the spleen, as well as to identify the translational connections between these subsets. The Monocle2 function for plotting pseudotime heatmaps was utilized to identify the significant role of different genes in the differentiation process. Genes with a q-value < 0.01 were deemed significantly altered and were detected using the differential GeneTest function in Monocle2.

Enzyme-linked immunosorbent assay (ELISA)

Mouse blood was drawn into EDTA tubes, centrifuged (3000 rpm, 10 min), and plasma was stored at -80 °C. According to the manufacturer's guidelines, plasma concentrations of anti-dsDNA antibodies, C3, and creatinine were determined using a Mouse ELISA Kit from Jingmei Biotechnology, China.

Renal histological analysis

Kidneys were harvested when the mice were euthanized after the administration of ApoBDs. Each kidney was divided in half, with one portion preserved in 4% paraformaldehyde in PBS, then embedded in paraffin and sliced into 4 μm sections. The sections were dyed using hematoxylin and eosin (H&E) and periodic acid–Schiff (PAS). As outlined in reference [23], the quantification of renal histopathological changes was performed. In brief, glomerular pathology was evaluated by analyzing 20 glomerular cross-sections from each kidney, with each glomerulus being rated on a semiquantitative scale considering factors like glomerular hypercellularity, mesangial matrix expansion, lymphocytes infiltration, focal necrosis, hyalinosis and crescent formation.

For indirect immunofluorescence assessment of IgG and C3 deposits in kidney tissues, sections were incubated with the anti-C3 antibody and anti-IgG (Abcam, USA) overnight at 4 °C. After washing off the primary antibodies, sections were stained with FITC-conjugated secondary antibodies at room temperature for 2 h. They were finally observed under a Zeiss microscope.

Lung histological analysis

The lungs were harvested when the mice were euthanized after the administration of ApoBDs. Each lung tissue was divided in half, with one portion preserved in 4% paraformaldehyde in PBS, then embedded in paraffin and sliced into 3 μm sections. The samples were dyed using H&E. The assessment and grading of inflammatory cell infiltration into tissues were conducted using this scale: 0 = no inflammatory cell presence; 1 = fewer than 10 cells detected; 2 = fewer than 20 cells observed; 3 = more than 20 cells identified. All the sections were assessed by a pathologist. The pathologist, who was not given any information about the trial groups, assessed five sections per animal [24].

Flow cytometry analysis for lymphocytes and macrophages in spleen

The single-cell suspension was created from spleen samples to conduct the flow cytometry experiments. Splenocytes were unfrozen, resuspended with FACS buffer, washed and centrifuged (700 g for 5 min at 4 °C) twice and resuspended with PBS and FBS. Each sample was incubated for 30 min in darkness at room temperature with a range of anti-mouse monoclonal antibodies (BD or Biosciences): Fixable viability stain (FVD)-455UV; F4/80-percp-cy5.5; CD86-FITC; CD206-PE; CD3-APC-cy7; CD4-FITC; CD25-PE; Foxp3-BV421; ICOS-BV605; PD-1-APC. Cells were treated with permeabilization buffer (Thermofisher, USA) to stain for intracellular Foxp3 following the guidelines provided by the manufacturer. Samples were examined on a FACS Calibur (BD fortessa, USA) and analyzed with Flowjo software.

Albuminuria

24-hour urine samples were gathered from each mouse using metabolic cages. Urinary albumin concentrations were determined with a commercially available ELISA kit (Solarbio, China), following the provided guidelines.

Statistical analysis

The statistical analysis was performed by GraphPad Prism version 8. For comparisons between two groups, two-tailed unpaired Student's t-tests were applied. Multiple group comparisons were analyzed by either one-way or two-way analysis of variance (ANOVA). The difference between groups was considered statistically significant for $^{*}p < 0.05$.

Results

Generation and characterization of M2 macrophages and derived-ApoBDs

To gain macrophages and derived-ApoBDs, we differentiated mononuclear cells from mouse bone marrow and activated macrophages (Fig. 1A). In brief, mononuclear cells extracted from the bone marrow of mouse tibia were cultured with macrophage colony-stimulating factor (M-CSF) for 7 days to develop into mature macrophages (M0 Mϕ). Macrophages showed relatively small and round in shape, with some protrusions (Fig. S1A). According to flow cytometry data, over 99% of bone marrow-derived mononuclear cells differentiated into F4/80-positive M0 Mϕ (Fig. S1B). We additionally activated the unpolarized M0 Mϕ with IL-4, showing a time- and concentration dependent manner (Fig. S2). Therefore, 100 μg/mL IL-4 and stimulation time of 48 h were used

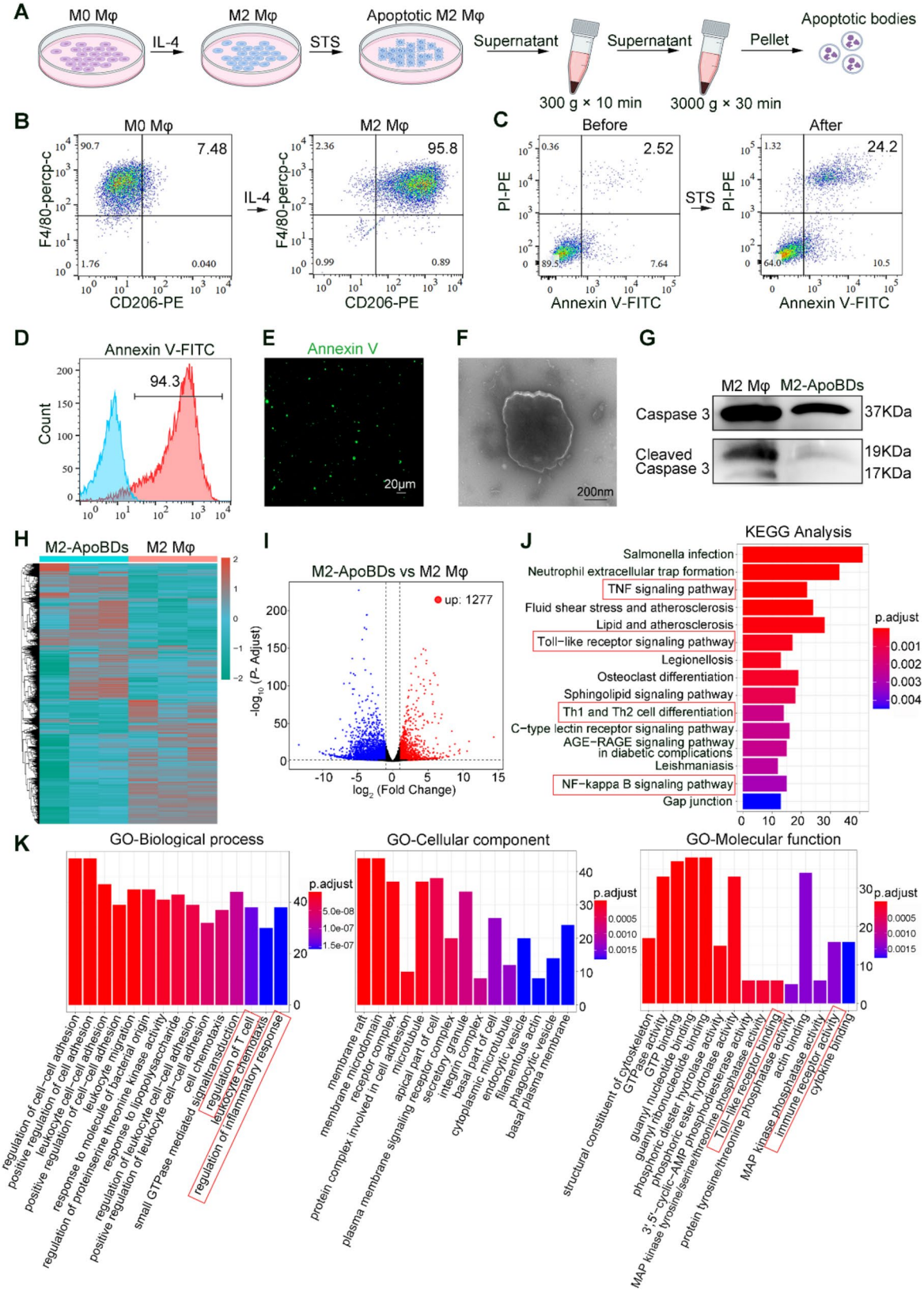

Fig. 1 (See legend on next page.)

(See figure on previous page.)

Fig. 1 Generation and characterization of M2 Mφ and derived-ApoBDs. (**A**) Schematic showed the purification of M2-ApoBDs through primary cell extraction, apoptosis induction and multiple centrifugations, as well as the production of ApoBDs. (**B**-**C**) Flow cytometric analysis showed that the proportion of M0, M2 Mφ and apoptotic Mφ. (**D**) Flow cytometric examination of Annexin V (green) staining in ApoBDs. (**E**) Representative microscopy images of Annexin V (green) staining in ApoBDs. Scale bars, 20 μm. (**F**) Representative TEM image of ApoBDs. Scale bars = 200 nm. (**G**) Western blotting analysis of M2 Mφ and derived-ApoBDs. (**H**) Heatmap representation of mRNA sequences between M2-ApoBDs and M2 Mφ (Fold change > 1 and *P* value < 0.05). (**I**) The volcano plot illustrates mRNAs that are significantly increased (red dots) and decreased (blue dots) in M2-ApoBDs relative to M2 macrophages (Fold change > 1, *P* value < 0.05). (**J**) KEGG pathway analysis of significantly upregulated mRNAs in M2-ApoBDs. (**K**) GO analysis of notably increased mRNAs in M2-ApoBDs, categorized into 'Cellular component', 'Molecular function' and 'Biological process'

to conducting the follow-up experiments. Flow cytometry showed that more than 95% of macrophages had been polarized to M2 macrophages ($F4/80^+CD206^+$) (Fig. 1B). To induce cell apoptosis, macrophages were washed with PBS and subsequently exposed to staurosporine (STS). Flow cytometry was employed to measure the apoptosis of macrophages (Fig. 1C, S3). ApoBDs were isolated from apoptotic macrophages by means of an enhanced density gradient centrifugation approach [25]. Subsequently, flow cytometry was employed to analyze Annexin V expression. Results showed that ApoBDs were mostly (above 94%) positive for Annexin V (Fig. 1D). Fluorescence staining was used to detect Annexin V expression, which revealed the exposure of phosphatidylserine (PS) (Fig. 1E). TEM showed that macrophages-derived ApoBDs were vesicles approximately 0.5 μm in diameter (Fig. 1F). NTA analysis results showed that the diameter peak value of ApoBDs was 522.5 nm (Fig. S4). Western blotting analysis were performed to demonstrate the presence of apoptosis-associated marker Caspase 3 and cleaved Caspase 3 (Fig. 1G). The molecular composition of EVs is a key area of interest in the field, as they carry various functional mRNA [26]. To pinpoint the specific mRNA features of M2 macrophages and derived-ApoBDs, we conducted transcriptome sequencing. A total of 3776 mRNA were identified (Fig. 1H), within which 1277 mRNAs were significantly upregulated in ApoBDs (Fig. 1I). Subsequently, we concentrated on these enhanced genes and performed a functional evaluation. Firstly, we investigated the pathways associated with the upregulated mRNAs using Kyoto Encyclopedia of Genes and Genomes (KEGG) pathway analysis. Findings indicated that these mRNAs were linked to the 'TNF signaling pathway', 'Toll – like receptor signaling pathway', 'Th1 and Th2 cell differentiation' and 'NF – kappa B signaling pathway', participating in the process of immune regulation and inflammatory response (Fig. 1J). Regarding the functional annotations derived from Gene ontology (GO) database, the upregulated genes were categorized into several terms across the three domains: 'Biological process', 'Cellular component', and 'Molecular function', indicating a variety of functional mRNA present in ApoBDs (Fig. 1K). Analysis of enrichment indicated that M2-ApoBDs exhibited elevated mRNA expression with regulatory functions, such as 'regulation of T cells' and 'regulation of inflammatory response'. Furthermore, results of molecular function enrichment analysis showed that these genes were associated with 'Toll – like receptor binding' and 'immune receptor activity'. The results indicate that M2-ApoBDs, which are rich in functional mRNAs closely associated with immune regulation and inflammatory response, have the potential to regulate the function of immune cells.

ApoBDs were preferentially enriched in spleen and selective taken up by spleen macrophages

The spleen, a crucial organ of the immune system, is vital for the clearance of apoptotic cells, the activation of immune cells, and the production of autoantibodies [27]. Dysregulated activation of immune cells in the spleen is linked to the pathogenesis of SLE [28]. To investigate the spleen-specific targeting capability of ApoBDs, we detected the distribution of administered ApoBDs in MRL/lpr mice model at 2 h, 6 h, 12 h and 24 h (Fig. S5). Ex vivo fluorescence imaging of organs showed significant accumulation of ApoBDs in spleen at 24 h post-injection, second only to the liver (Fig. 2A, B). To explore the selective cellular targeting ability, flow cytometry analysis revealed that spleen macrophages engulfed a higher percentage of ApoBDs compared to $CD4^+$T cells, $CD8^+$T cells and B cells (73.4% vs. 7.93% vs. 3.13% vs. 9.73%) (Fig. 2C, S6). The tissue fluorescence results further confirmed accumulation of ApoBDs in the spleen macrophages at 24 h post-injection (Fig. 2D). In summary, these findings indicated the remarkable targeting ability of ApoBDs to spleen tissue and the specific uptaken by macrophages just as we expected.

M2-ApoBDs induced functional changes in spleen macrophages in MRL/lpr mice

Previous studies have demonstrated that ApoBDs can significantly influence the immune response in macrophages [29]. To further study the immune regulation effect of M2-ApoBDs on macrophages in SLE, we administered M0 and M2-ApoBDs via tail vein injections to 10-week-old MRL/lpr mice weekly for 8 weeks. Single-cell suspension of the spleens was profiled with scRNA-seq. Based on specifically upregulated gene signatures in each cluster, 9 major cell types were identified [30]: Basophils (Cpa3, Ms4a2), NK cells (Ncr1, Klrd1), Dendritic cells (Olfm1, Xcr1, Clec9a), Plasma cells (Igkc, Jchain), Macrophages (CD68, C1qb, C1qc), Neutrophils

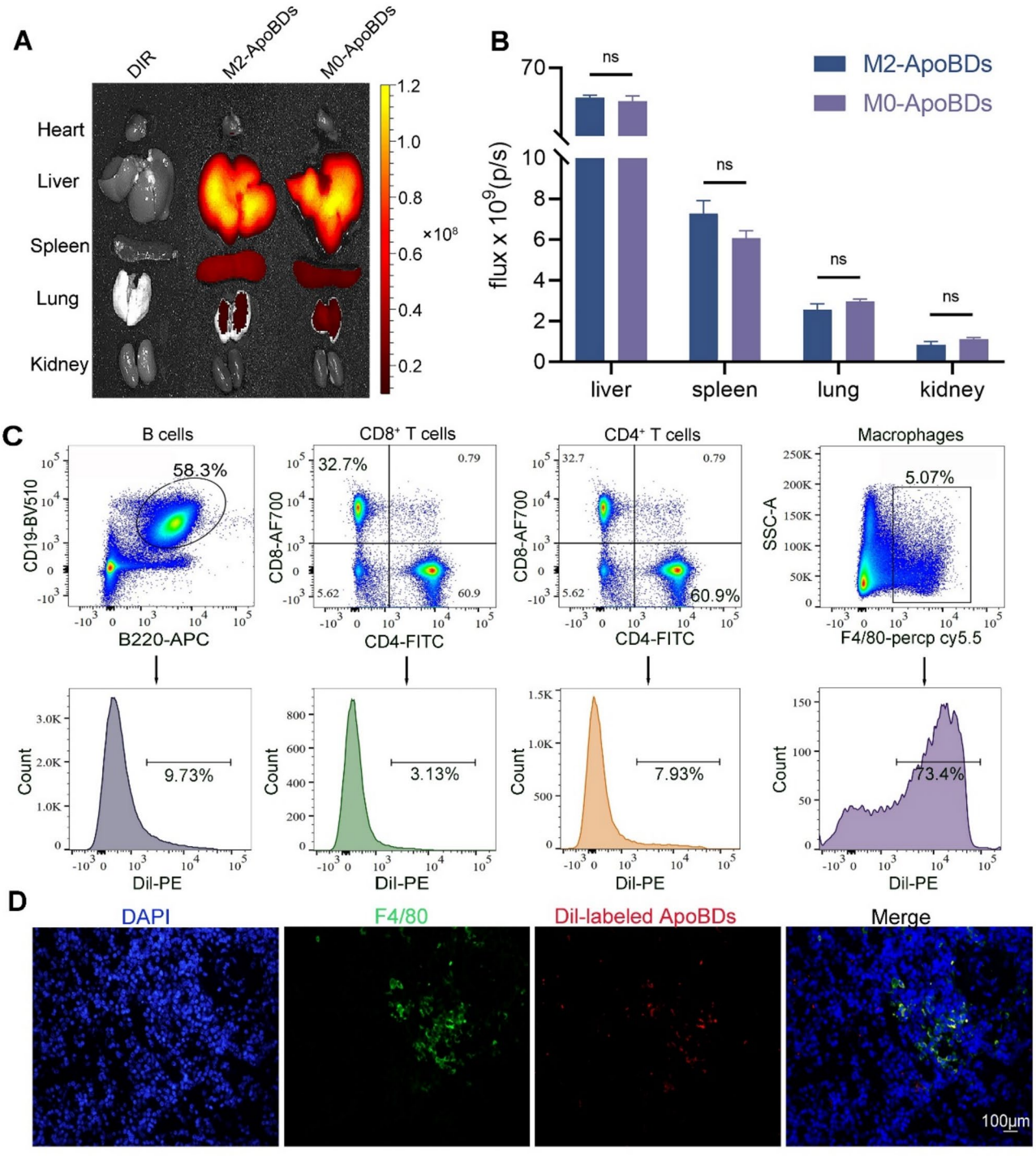

Fig. 2 ApoBDs were preferentially enriched in spleen and selective taken up by macrophage. (**A**) Ex vivo fluorescence imaging of the major organs 24 h after injection of DiR-labeled ApoBDs. (**B**) Quantification of average fluorescence units in organs of lung, liver and spleen. The color scale corresponds to radiant efficiency [(p/sec/cm2/sr)/(μW/cm2)]. (**C**) Flow cytometric analysis showed the uptake of Dil-labeled ApoBDs by macrophages, $CD4^+$T cells, $CD8^+$T cells and B cells in the spleen. (**D**) Representative immunofluorescent (IF) staining images of F4/80 (green) and Dil-labeled ApoBDs (red) in the spleen, counterstained by DAPI (blue). Scale bars, 100 μm

(Camp, Cxcl2, Retnlg), Erythrocytes (Hba-a2, Hba-a1), B cells (Ms4a1, CD19, CD79a), T cells (CD3g, CD3e, CD3d) (Fig. 3A-B). To explore the change of gene expression in macrophages cluster, a volcano plot and heatmap showing specific differentially expressed genes (DEGs) were created (Fig. 3C-D). Results showed that compared with that of M0-ApoBDs treatment group, 15 genes exhibited up-regulated expression, while 74

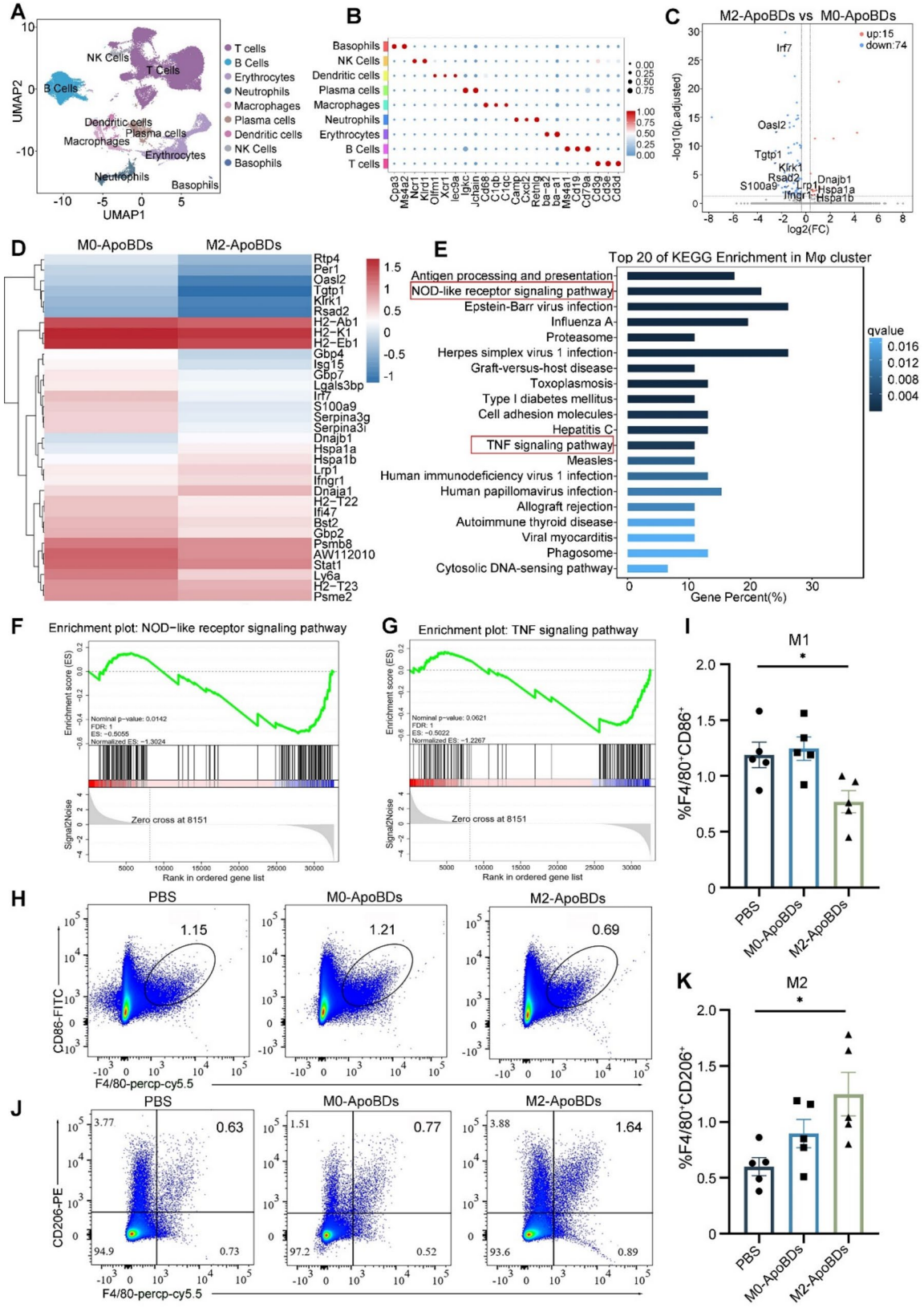

Fig. 3 (See legend on next page.)

(See figure on previous page.)

Fig. 3 M2-ApoBDs induced functional changes in spleen macrophages in MRL/lpr mice. (**A**) UMAP analysis showed that there were 9 different cell clusters in the spleen. Different cell clusters are color-coded. (**B**) Expression levels of cell marker genes used to define 9 cell clusters. (**C**) Volcano plot showing significantly up-regulated (red dots) and down-regulated (blue dots) mRNAs in spleen macrophages of M2-ApoBDs compared to M0-ApoBDs (Fold change > 0.2, *P* value < 0.05). (**D**) Heatmap representation of mRNA sequences in spleen macrophages between M2-ApoBDs and M0-ApoBDs treatment group (Fold change > 0.2 and P value < 0.05). (**E**) KEGG pathway analysis of significantly down-regulated mRNAs in macrophages from M2-ApoBDs treatment group. (**F**-**G**) GSEA-KEGG analysis showed 'TNF signaling pathway' and 'NOD-like receptor signaling pathway' were down-regulated in M2-ApoBDs treatment groups. (**H**-**I**) Flow cytometric analysis showed the proportion of F4/80$^+$ CD86$^+$ cells in spleen after M2-ApoBDs or M0-ApoBDs administration. (**J**-**K**) Flow cytometric analysis showed the proportion of F4/80$^+$ CD206$^+$ cells after M2-ApoBDs or M0-ApoBDs administration. Statistical analysis was processed using a one-way ANOVA with multiple comparison test ($^*p < 0.05$)

genes showed down-regulated expression in the macrophage cluster of M2-ApoBDs treatment group (Fold change > 0.2, $p < 0.05$). Several genes with the potential to induce inflammation were down-regulated, including Tgpt1 (also known as Irgb6) [31], Oasl2 [32], Irf7 [33], S100a9 [34], Rsad2 [35], Klrk1 [36], and anti-inflammatory genes are up-regulated, including Hspa1a (also known as Hsp72) [37], Dnajb1 [38], Lrp1 [39], Ifngr1 [40]. Significantly, Tgpt1, Oasl2 and Irf7 were important immune-related genes that played a crucial role in the functional regulation of macrophages [41]. The expression of Irf7 is closely related to the polarization state of macrophages, and it may influence the immune pathological processes of SLE by regulating macrophage activity [42]. Then, we investigated the pathways associated with DEGs between M0-ApoBDs and M2-ApoBDs treatment groups via KEGG pathway analysis. KEGG enrichment analysis showed that several inflammatory-related pathways, e.g. 'TNF signaling pathway' and 'NOD-like receptor signaling pathway' were highly enriched for these downDEGs in macrophages from M2-ApoBDs treatment groups (Fig. 3E). GSEA results of KEGG terms further revealed that 'TNF signaling pathway' and 'NOD-like receptor signaling pathway' were down-regulated in M2-ApoBDs treatment groups (Fig. 3F-G). 'T cell signaling pathway' and 'TGF-β signaling pathway' were up-regulated in M2-ApoBDs treatment groups, which reminded us that reprogrammed macrophage might interact with T cells, especially Treg cells (Fig. S7A-B). M1-like (pro-inflammatory) and M2-like (anti-inflammatory) macrophages are the two extremes on this functional spectrum, so we checked the effects of ApoBDs on macrophage M1/M2 polarization by using flow cytometry (Fig. S8). The percentage of M1 macrophages (F4/80$^+$CD86$^+$) in spleen after treatment with M2-ApoBDs was down-regulated, compared to M0-ApoBDs and non-intervention treatment group, by using flow cytometry (Fig. 3H-I). Meanwhile, the percentage of M2-like macrophage (F4/80$^+$CD206$^+$) was significantly up-regulated (Fig. 3J-K). These results indicated that targeting delivery of M2-ApoBDs leaded to transcriptional reprogramming of macrophages in spleen of MRL/lpr mice.

M2-ApoBDs induced M2-like (anti-inflammatory) reprogramming of macrophages in vitro

We firstly assessed the efficiency of the uptake of ApoBDs and found that ApoBDs could be up-taken by macrophages at 6 h and 12 h (Fig. 4A; Fig. S9). To verify whether M2-ApoBDs can trigger the M2 reprogramming in macrophages, 100ng/mL LPS pre-stimulated BMDMs were used to mimic SLE macrophages firstly (Fig. S10), then we incubated macrophages with ApoBDs at concentration gradients of 0–100 μg/mL for 24 h to observe the effect of ApoBDs on reprogramming of macrophages. Flow cytometry method was used to detect the percentage of F4/80$^+$ CD206$^+$ cells, showing that the percentage of M2 reached 75.4% at a concentration of 10 μg/mL when incubated with M2-ApoBDs, and this significantly increased to 86.2% at 100 μg/mL ApoBDs (Fig. 4B, C). Therefore, the 100 μg/mL concentration of M2 ApoBDs were selected to conduct the following experiments. Western blot results showed that CD206 protein expression level in macrophages after M2-ApoBDs incubation increased, while the protein expression levels of iNOS and CD86 decreased (Fig. 4D, E). QRT-PCR results were consistent with previous Western blot experiments (Fig. 4F-I). Elisa results showed the expressions of TNF-α and IL-6 were down-regulated in M2-ApoBDs-cocultured group (Fig. 4J, K). These results indicate that macrophages can be successfully reprogrammed into M2-like (anti-inflammatory) macrophages by M2- ApoBDs-guided phenotypic switch.

M2-ApoBDs promoted the differentiation of Treg cells in MRL/lpr mice

Macrophages are crucial in regulating adaptive immune response, especially T cell immune regulation. Macrophages are capable of facilitating and delivering the essential costimulatory signaling and cytokine release necessary for T cell activation [43]. Quantitative and functional impairments of Treg cells have been observed in numerous autoimmune disorders, especially SLE [44]. According to the recently published single-cell data of immune canonical markers [45], T cells were categorized into 14 clusters (Fig. 5A). Expression levels of 14 T cell clusters marker genes were showed in Fig. S11. To discover the effect of M2-ApoBDs on T cell differentiation, we carried out the pseudo-time analysis of T cell clusters.

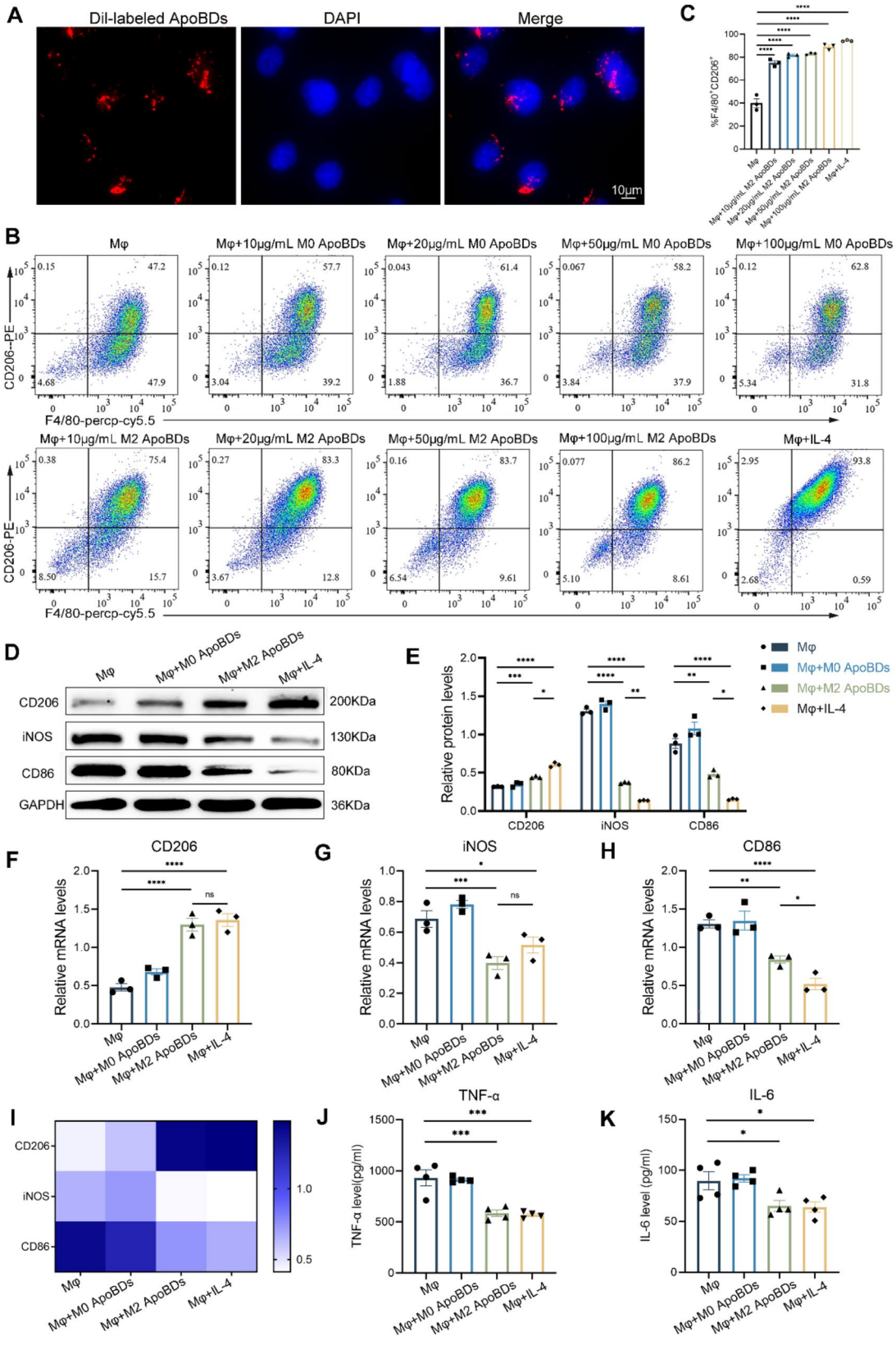

Fig. 4 (See legend on next page.)

(See figure on previous page.)

Fig. 4 M2-ApoBDs induced M2-like (anti-inflammatory) reprogramming of macrophages in vitro. (**A**) fluorescence images of Mφ incubation with of Dil-labeled ApoBDs (Red) at 6 h. Scale bars, 10 μm. (**B**-**C**) Flow cytometric analysis showed the proportion of F4/80 + CD206 + cells after M2-ApoBDs or M0-ApoBDs incubation. (**D**-**E**) Western blot analysis of Mφ treated with 100 μg/mL of M2-ApoBDs or M0-ApoBDs. (**F**-**G**) Relative gray value of CD206, iNOS and CD86 in Mφ. (**H**-**J**) Relative mRNA expression of CD206, iNOS and CD86 in Mφ. (**I**) Heat map for expression analysis (using RT-qPCR) of CD206, iNOS and CD86. (**J**-**K**) Elisa was used to detect the levels of of TNF-α and IL-6 in ApoBDs and macrophages cocultured supernantant. Statistical analysis was processed using a one-way or two-way ANOVA with multiple comparison test ($^{*}p < 0.05$, $^{**}p < 0.01$, $^{***}p < 0.001$, $^{****}p < 0.0001$)

As shown in Fig. 5B, the trend of Treg differentiation was obvious in active stage. In order to further examine the changes in gene expression, we performed pseudo-time analysis on the single cells. Foxp3, a marker of Treg cells, showed relatively high expression in M2-ApoBDs-treated group (Fig. 5C, D). Therefore, we supposed that the treatment of M2-ApoBDs could promoted the differentiation of Treg cells in MRL/lpr mice. Then, we performed the transcriptome analysis of Treg cluster and identified 11 upregulated genes and 15 downregulated genes, including Irf7, S100A9 and Danjb, which were also included in the differential genes of macrophage cluster (Fig. 5E, F). These results reminded us that reprogrammed macrophages could regulate Treg cell differentiation through intercellular interaction. With regard to the functional analysis based on KEGG database, the DEGs in Treg cluster were associated with immunity and inflammation, including 'NOD-like receptor signaling pathway', 'PI3K-Akt signaling pathway', 'IL-17 signaling pathway', and 'Toll-like receptor signaling pathway' (Fig. 5G). GSEA results revealed that 'TGF-β signaling pathway' was up-regulated in M2-ApoBDs treatment groups (Fig. 5H). We also sought to assess the effect of ApoBDs treatment on Treg cells via flow cytometry analysis. Our investigations showed that the proportion of Treg cells and $ICOS^+$ Treg cells in spleen were increased after M2-ApoBDs injection (Fig. 5I-L).

M2 macrophages reprogrammed by M2-ApoBDs promoted the differentiation of Treg cells in vitro

Macrophages can modulate T cell suppression via direct interaction and the release of cytokines and metabolic byproducts [46]. To determine whether reprogrammed macrophages regulated the differentiation of Treg cells, we established the flow cytometry panel of Treg cells (Fig. S12A) and cocultured splenocytes with macrophages after incubated with M2-ApoBDs or M0-ApoBDs. Our observations revealed that the proportion of Treg cells increased when cocultured with macrophages after incubated with 10–100 μg/mL M2-ApoBDs in direct coculture (Fig. S12B). To discover the contact dependent manner between macrophage and T cells, we used two cell culture methods of direct coculture and trans-well coculture. As the result showed, the proportion of Treg cells increased cocultured splenocytes with macrophages after incubated with M2-ApoBDs in direct coculture (Fig. 6C-H), not in trans-well coculture manner (Fig. 6A, B), which indicated that macrophages might promote the differentiation of Treg cells through receptor-ligand interaction. ICOS (inducible T-cell co-stimulator) and PD-1 (programmed cell death protein 1), as costimulatory molecules, regulate Treg cells expansion [47]. Therefore, we detected the percentage of $ICOS^+$ Treg cells and PD-1^+ Treg cells after cocultured with macrophages. The percentage of $ICOS^+$ Treg cells elevated significantly after cocultured with M2 macrophages. However, the proportion of PD-1^+Treg cells showed no statistical difference. Taken together, M2 macrophages triggered the differentiation of Treg cells in direct contact manner. To investigate intercellular receptor-ligand interaction, we used CellChat to explore cell-cell communications between macrophages and other immune cells. It was found that macrophages might interact with Treg cells via APP-CD74 ligand-receptor pairs in the M2-ApoBDs treatment group (Fig. 6I-J).

Multiple mRNAs were up-regulated in M2-ApoBDs compared to M0-ApoBDs, of them, Mgl2 played a vital role

ApoBDs have been shown to carry functional mRNA cargos to recipient cells, thus play an important role in intercellular communication [48]. We assessed whether M2-ApoBDs could carry functional mRNAs, which would lead to mRNA expression in macrophages that internalize them. Therefore, ApoBDs isolated from M0 macrophages and M2 macrophages were subjected to mRNA sequencing (Fig. 7A). A total of 469 differentially expressed mRNAs were identified, including 113 up-regulated mRNAs in M2-ApoBDs (Fig. 7B). The top 4 up-regulated mRNAs (Ccl8, Rnase2a, Mgl2 and Chil3) were selected for preliminary validation. Of them, the expression of Mgl2 was significantly upregulated in M2-ApoBDs compared with M0-ApoBDs (Fig. 7C). To further discover the relationship between Mgl2 and Macrophage phenotype, we transfected macrophages with Mgl2 siRNA or negative control (NC). According to the transfection efficiency, si-Mgl2 4# was selected for the next experiment (Fig. S13A). The results of qRT-PCR indicated that si-Mgl2 4# significantly reduced CD206 expression and induced iNOS expression (Fig. S13B, C). We then examined the impact of si-Mgl2 on inflammation. The application of Mgl2 siRNA to macrophages led to a notable augmentation in TNF-α and IL-6 (Fig. S13D-E). There was no statistical difference in the expression of IL-1β, but there was an upward trend

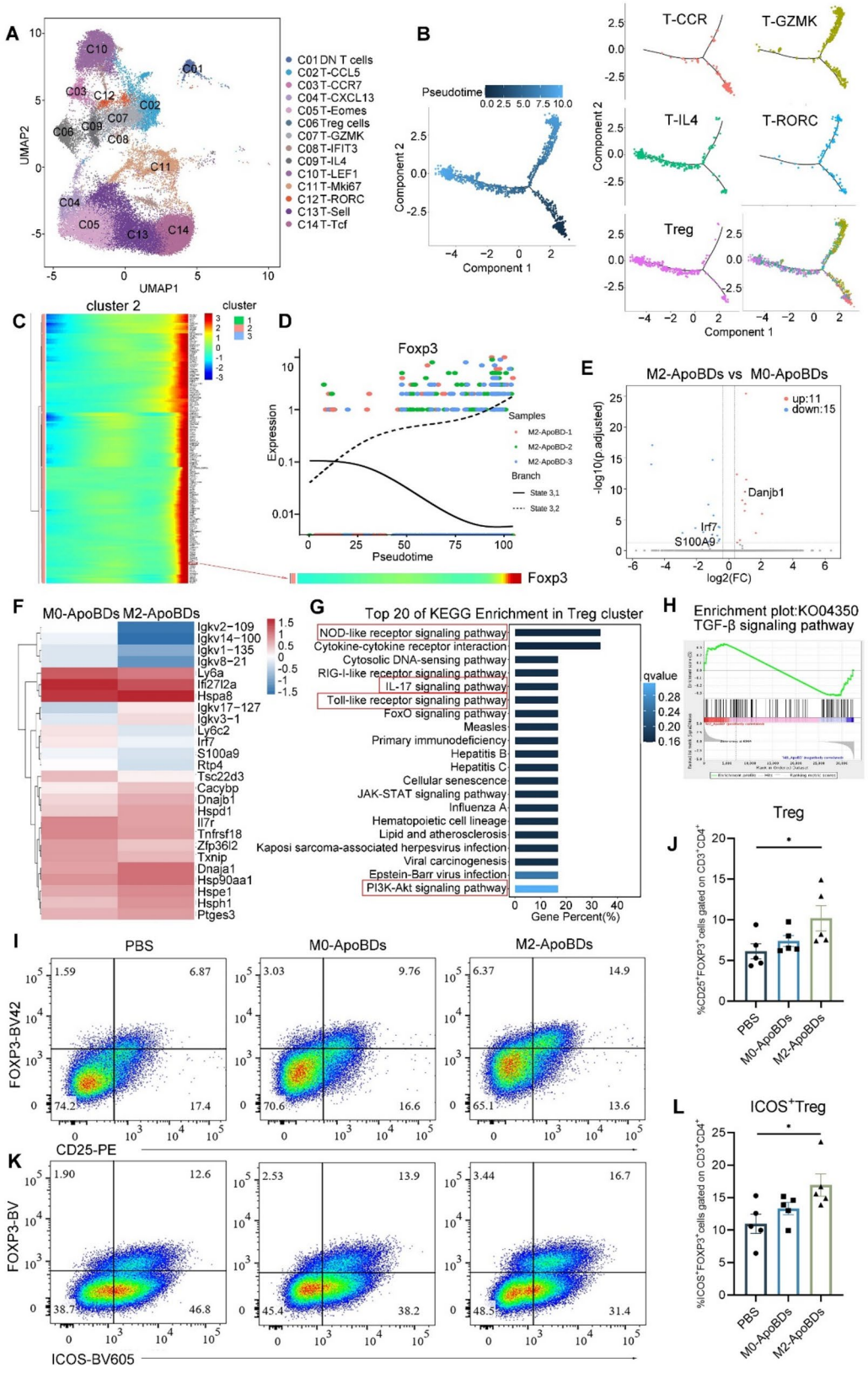

Fig. 5 (See legend on next page.)

(See figure on previous page.)

Fig. 5 M2-ApoBDs promoted the differentiation of Treg cells in MRL/lpr mice. (**A**) UMAP analysis showed that there were 23 different cell clusters in the spleen. Different cell clusters are color-coded. (**B**) Pseudo-time analysis of T cell clusters. (**C**-**D**) The expression of Foxp3 was upregulated as T cells differentiated. (**E**) Volcano plot showed significantly upregulated (red dots) and downregulated (blue dots) mRNAs in spleen Treg cells of M2-ApoBDs compared to M0-ApoBDs (Fold change > 0.2, *P* value < 0.05). (**F**) Heatmap representation of mRNA sequences in spleen Treg cluster between M2-ApoBDs and M0-ApoBDs treatment group (Fold change > 0.2 and *p* value < 0.05). (**G**) KEGG pathway analysis of significantly downregulated mRNAs in Treg cells from M2-ApoBDs treatment group. (**H**) GSEA-KEGG analysis showed 'TGF-β signaling pathway' was up-regulated in M2-ApoBDs treatment groups. (**I**-**J**) Flow cytometric analysis showed the proportion of Treg cells after M2-ApoBDs or M0-ApoBDs administration. (**K**-**L**) Flow cytometric analysis showed the proportion of $ICOS^+$ Treg cells after M2-ApoBDs or M0-ApoBDs administration. Statistical analysis was processed using a one-way ANOVA with multiple comparison test ($^*p < 0.05$)

(Fig. S13F). Therefore, Mgl2 played a vital role in macrophage reprogramming. KEGG pathway analysis revealed upregulated-DEGs in M2-ApoBDs were linked to cellular behavior, signaling transduction and immune regulation, such as 'Chemokine signaling pathway', 'Cytokine – cytokine receptor interaction' and 'Antigen processing and presentation' (Fig. 7D). Similarly, concerning the 'Molecular function' category in GO database, there was an obvious enrichment of DEGs linked to cellular behavior, signaling transduction, including 'chemokine activity', 'CCR chemokine receptor binding', 'chemokine receptor binding' and 'receptor ligand activity'. These data indicated that multiple functional mRNAs were up-regulated in M2-ApoBDs compared to M0-ApoBDs, among them, Mgl2 played a vital role.

Administration of M2-ApoBDs improved SLE clinical manifestation

To determine whether increased M2-ApoBDs accumulation in spleen and subsequent macrophages polarization to Treg immune regulation could further ameliorate SLE, 10-week-old MRL/lpr mice were tail vein injected M0 and M2-ApoBDs once a week for 8 weeks (Fig. 8A). At 18 weeks, blood, kidneys, lungs, and spleens were collected from all mice. Our findings indicated that M2-ApoBDs significantly decreased the levels of albuminuria and creatinine in MRL/lpr mice, but M0-ApoBDs did not (Fig. 8B, C). Complement C3 and anti-dsDNA autoantibody are commonly associated with lupus activity, so we measured their levels using ELISA Kits. The level of anti-dsDNA was decreased in M2-ApoBDs-treated group (Fig. 8D). Although the level of C3 did not reach statistical difference, there was an upward trend in M2-ApoBDs-treated group (Fig. 8E). We think that the expression trend of C3 was meaningful. The small sample size, individual variations and the timing of detection might explain why plasma C3 levels did not show statistically significant differences. HE staining of the lung sections revealed M2-ApoBDs reduced interstitial lung inflammation and the histologic score (Fig. 8F, G). Results of H&E and PAS staining revealed that M2-ApoBDs therapy downregulated immune cell infiltration in the kidney interstitium and lessened glomerular mesangial enlargement (Fig. 8H-J). The application of M2-ApoBDs significantly decreased glomerular C3 and IgG depositions in kidney compared to M0-ApoBDs and non-intervention group (Fig. 8K, L). The complement C3 might be primarily activated locally in the kidneys without entering the systemic circulation in large quantities, which could explain why plasma C3 levels did not show statistically significant differences, but the immunofluorescence results show significant differences. A toxicity assessment was performed in normal mice following the administration of M0 and M2-ApoBDs. Histological analysis showed no obvious acute organ damage in any of the treated groups (Fig. S14). Overall, the findings indicated that M2-ApoBDs with improved immunomodulatory properties could serve as a safe and effective treatment option for SLE.

Discussion

In this study, we successfully isolated M2-ApoBDs which could be captured by spleen tissue, especially spleen macrophages, which provided a possibility to regulate the polarization of macrophages. The efferocytosis of M2-ApoBDs induced transcriptional reprogramming of M2 macrophages, then induced-M2 macrophage enhanced the differentiation of Treg cells in cellular direct contact. Systemic administration of M2 macrophages derived-ApoBDs could alleviate the development of SLE by macrophage reprogramming and Treg differentiation. Taken together, M2-ApoBDs represents a promising strategy for SLE therapy.

Targeted immune therapy is an attractive strategy for autoimmune disease, including SLE [49, 50]. Although EVs from living cells have received substantial attention recently, our knowledge about ApoBDs generated by apoptotic cells remains quite limited [16]. During cell apoptosis, ApoBDs are uniquely formed to encapsulate cellular components produced in the process. PtdSer recognition receptors are crucial for identifying and engulfing apoptotic bodies [51]. Antigen-presenting cells such as macrophages phagocytose apoptotic bodies, presenting antigens to the immune system to modulate T cell responses. ApoBDs possess characteristics such as high stability, biocompatibility, immunogenicity, and precise targeting, making them a promising option for immunotherapy [52]. Previous study showed that apoptotic vesicles derived from MSCs could reprogram macrophages at the transcriptional level through efferocytosis, reduce

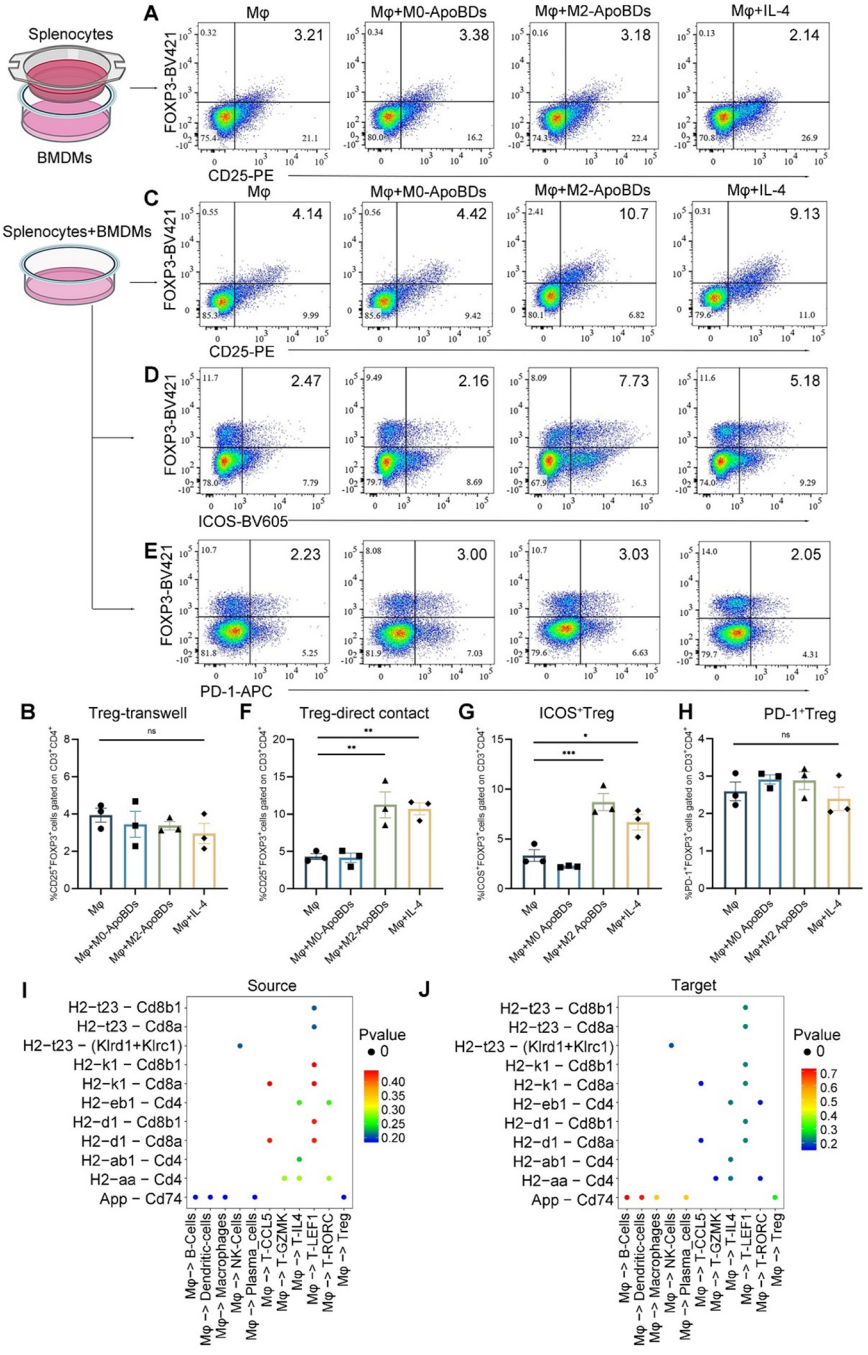

Fig. 6 M2 macrophages reprogrammed by M2-ApoBDs enhanced the differentiation of Treg cells in vitro. (**A**-**B**) Flow cytometric analysis showed the proportion of Treg cells transwell cocultured splenocytes with Mφ after incubated with M2-ApoBDs or M0-ApoBDs. (**C**-**D**) Flow cytometric analysis showed the proportion of Treg cells direct cocultured splenocytes with Mφ after incubated with M2-ApoBDs or M0-ApoBDs. (**E**-**F**) Flow cytometric analysis showed the proportion of ICOS^{+} Treg cells direct cocultured splenocytes with Mφ after incubated with M2-ApoBDs or M0-ApoBDs. (**G**-**H**) Flow cytometric analysis showed the proportion of PD-1^{+}Treg cells cocultured splenocytes with Mφ after incubated with M2-ApoBDs or M0-ApoBDs. (**I**-**J**) CellChat was used to analyze the relationship between immune-related ligands and receptors to predict the interaction between macrophages and other immune cells. Statistical analysis was processed using a one-way ANOVA with multiple comparison test ($^{*}p < 0.05$, $^{**}p < 0.01$, $^{***}p < 0.001$)

macrophage accumulation and improve type 2 diabetes [53]. Neutrophil apoptotic bodies, actively targeted to macrophages, could alleviate myocardial infarction by enhancing macrophage efferocytosis and resolving inflammation [54]. Our study demonstrated that ApoBDs could selectively target and localize to the spleen, second only to the liver. The liver, as a key organ for drug metabolism and a site rich in macrophages (e.g. Kupffer

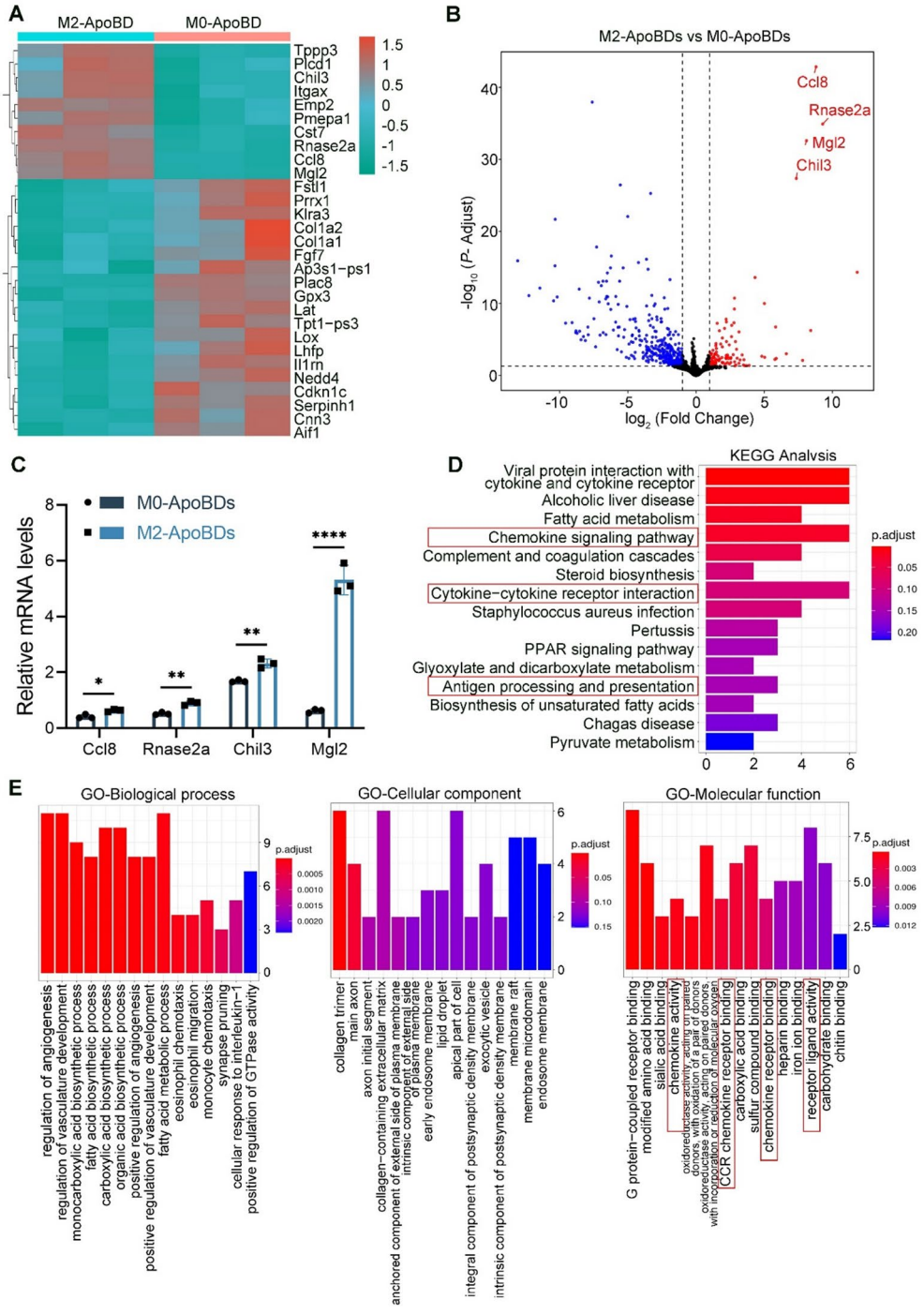

Fig. 7 Multiple mRNAs were up-regulated in M2-ApoBDs compared to M0-ApoBDs, of them, Mgl2 played a vital role. (**A**) Heatmap representation of mRNA sequences between M2-ApoBDs and M0 ApoBDs. (**B**) Volcano plot showing significantly upregulated (red dots) and downregulated (blue dots) mRNAs in M2-ApoBDs compared to M0 ApoBDs (Fold change > 1, $p < 0.05$). (**C**) The expression of Ccl8, Rnase2a, Chil3 and Mgl2 in M2-ApoBDs and M0 ApoBDs by qRT-PCR. (**D**) KEGG pathway analysis of upregulated mRNAs in M2-ApoBDs. (**E**) GO analysis of upregulated mRNAs in M2-ApoBDs, categorized into 'Cellular component', 'Molecular function' and 'Biological process'. Statistical analysis was processed using a one-way ANOVA with multiple comparison test ($^{*}p < 0.05$, $^{**}p < 0.01$, $^{****}p < 0.0001$)

cells), is capable of engulfing apoptotic bodies and other nanoparticles. The spleen and liver sequester most of administered nanoparticles, including apoptotic bodies, preventing them from entering the diseased tissue. Therefore, they may be the main barrier in the treatment of some diseases using nanomedicine, such as tumors or cardiovascular disease. However, it represents a great opportunity to therapeutically target splenocytes for

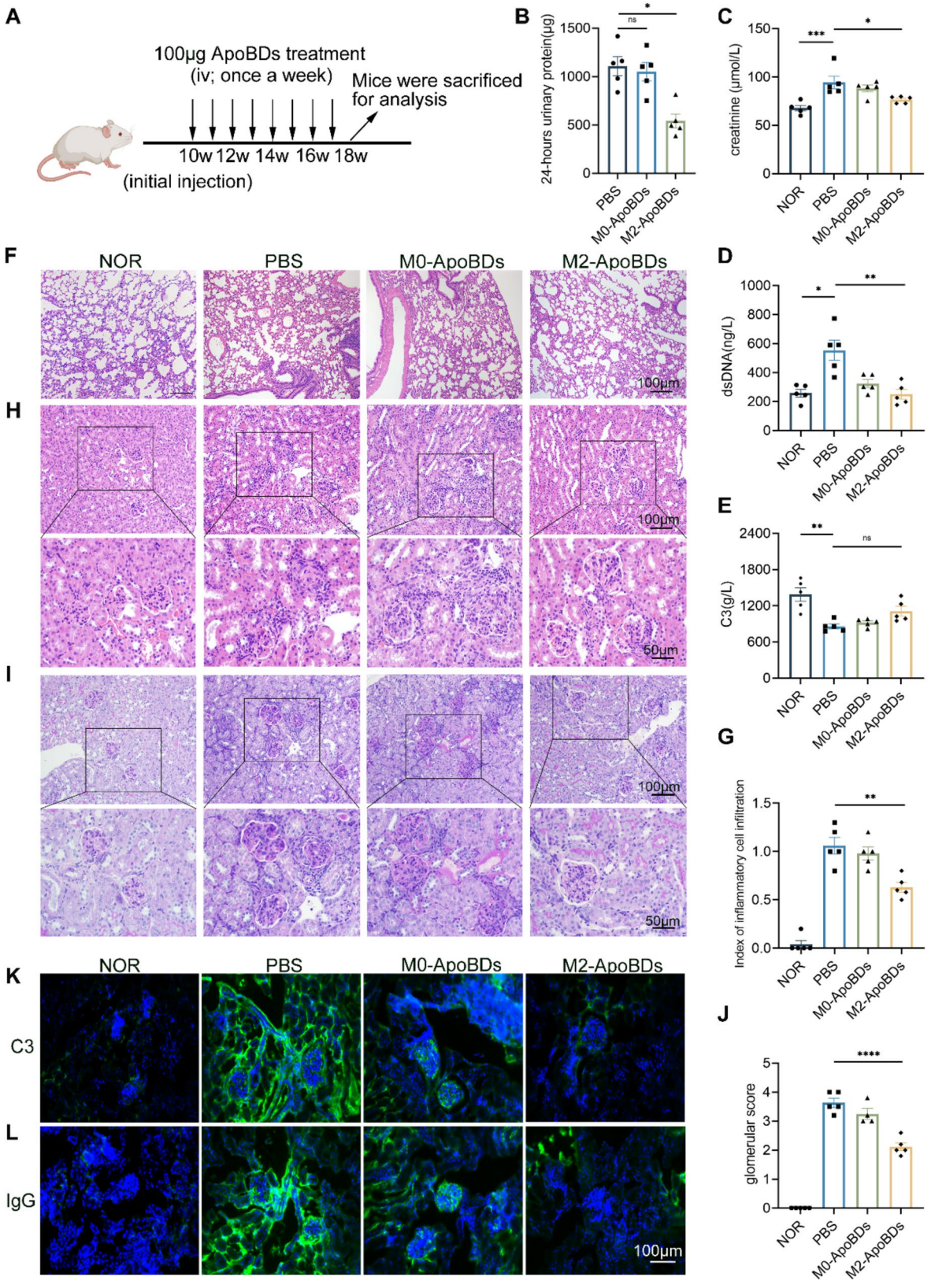

Fig. 8 (See legend on next page.)

(See figure on previous page.)

Fig. 8 Administration of M2 macrophages derived-ApoBDs improved SLE clinical manifestation. (**A**) Flowchart of mice ApoBDs treatment. (**B**) 24-hours urinary protein was measured by coomassie brilliant blue method. (**C**-**E**) Elisa was used to detect the levels of creatinine, C3 and anti-dsDNA. (**F**-**G**) Representative photographs of lung sections stained with HE. Scale bar: 200 μm. (**H**-**J**) Representative photographs of kidney sections stained with HE, PAS. Scale bar: 50 μm and 100 μm. (**K**-**L**) Immunofluorescence staining for mouse IgG and C3. Scale bar: 100 μm. Statistical analysis was processed using a one-way ANOVA with multiple comparison test ($^{*}p < 0.05$, $^{**}p < 0.01$, $^{****}p < 0.0001$)

treating SLE [55]. The spleen plays a central role in maintaining immune tolerance by clearing apoptotic cells, inducing Treg differentiation, and suppressing autoreactive T cells. Dysregulation of the spleen contributes to lupus [56]. Making targeting splenic immunoregulatory mechanisms provides a promising new direction for lupus therapy. Therefore, we further explore the target cells of apoptotic bodies in the spleen. Flow cytometry analysis revealed splenic macrophages have higher uptake efficiency (73.4%) compared to T cells and B cells. This finding suggested a potential role for ApoBDs in SLE therapy.

Macrophages, innate immune cells present in nearly all tissues, play a pivotal role in initiating, sustaining, and resolving inflammation. Their functions critically influence tissue damage or repair, and immune regulation [57]. The effects of macrophages are associated with the significant diversity and plasticity among various phenotypes. In brief, macrophages stimulated by specific microenvironmental signals can be categorized into two main types: M1 macrophages, which are classically activated and have pro-inflammatory properties, and M2 macrophages, which are alternatively activated and involved in anti-inflammatory responses and tissue repair [58, 59]. The polarization of macrophages is crucial for the progression and prognosis of autoimmune diseases, including SLE [6]. Dysregulation of macrophage phenotypes is known to play a pathogenic role in SLE. M1 macrophages are frequently appear in SLE with pro-inflammatory profiles [60]. Defective M2 macrophages could uncontrollably produce cytokines that contributed to the development of SLE [61]. This functional adaptability holds immense therapeutic value as it can be utilized to restore balance between different macrophage subtypes. Thus, the regulation of macrophages provides a potential approach for treating SLE [62]. Wei Huang et al. found that M2-ApoBDs could alleviate osteoarthritis progression by transforming M1 macrophages into a M2-like phenotype [63]. Our results showed that M2-ApoBDs could promote the transcriptional reprogramming of M2 (anti-inflammatory) macrophages via scRNA-seq in vivo and also in vitro, which provided an immunological basis in the treatment of SLE.

The reduction in the frequencies and malfunction of Treg cells are one of important mechanisms for the breakdown of peripheral tolerance and onset of SLE [64]. Enhancing self-tolerance by promoting functional Treg cells is a potential treatment for SLE [65]. Macrophages can regulate T cell immune through direct cellular interactions (e.g. Receptors-ligands) and through non-cellular direct contact (e.g. secretion of cytokines). Previous research showed that preprogrammed macrophages could enhance the functionality of Treg cells via the PD-L1-PD-1 pathway for autoimmune disease therapy [66]. Our experiments revealed that after incubated with M2-ApoBDs, M2 macrophages triggered the differentiation of Treg cells in direct contact coculture manner, which also reminded us that macrophages might promote the differentiation of Treg cells through receptor-ligand interaction. We used CellChat to study cell-cell communications between macrophages and other immune cells. It was found that macrophages might interact with Treg cells via APP-CD74 ligand-receptor pairs in the M2-ApoBDs treatment group. CD74 is a type II transmembrane glycoprotein, which is mainly involved in antigen presentation, inflammatory signal transduction and other processes, and can effectively promote the activation of $CD4^{+}$T cells [67]. The characteristics of macrophages can affect their capacity to display costimulatory or coinhibitory molecules, thereby regulating T cell activation or suppression [46].

However, there are a few limitations of our study. Our current study elucidated the immunoregulatory functions of ApoBDs and investigated the preliminary safety and efficacy of ApoBD-based therapy. A comprehensive evaluation of chronic toxicity would require large-scale animal studies with extended observation periods and specialized toxicological testing. Currently, we have completed preliminary safety assessments. Further research is essential to fully understand chronic toxicity, immune tolerance, and potential off-target effects of ApoBDs.

Conclusion

In summary, we collected M2 ApoBDs which were captured by spleen macrophages in vivo. Efferocytosis of ApoBDs could induce transcriptional reprogramming of spleen macrophages and then modulated Treg cells differentiation through this ligand-receptor interaction based on scRNA-seq. Because of targeted immune regulation function, systemic administration of M2-ApoBDs could alleviate the development of SLE. Overall, these findings not only provide promising employment for M2-ApoBDs in the treatment of SLE but also highlight the immune regulation potential of M2-ApoBDs for SLE, which enhances the possibility of M2-ApoBDs targeted immune therapy in clinical application. Therefore,

further research and clinical investigations are warranted to delve into the long-term effects of M2-ApoBDs in treating SLE.

Supplementary Information

The online version contains supplementary material available at https://doi.org/10.1186/s12951-025-03437-4.

Supplementary Material 1

Author contributions

JJ: conceptualization, data curation, investigation, writing– original draft, writing - review and editing. SY: investigation, methodology and funding acquisition. YX and QH: investigation, methodology, writing - review and editing. QLiang, GF, YX, MY, YH and JY: investigation, and methodology. CD, RZ and YW: data analysis and writing - review and editing. GG, XS and JL: data analysis and investigation. YG and ZG: conceptualization, experimental design, supervision, and writing- review and editing.

Funding

This work was supported by National Natural Science Foundation of China (82302053).

Data availability

All data are available from the corresponding authors upon reasonable request.

Declarations

Ethics approval and consent to participate

This study was approved by The Ethics Committee of Nantong University. All animal experiments were performed under animal research guidelines and an institutionally approved protocol at Nantong University (No. S20230818-002).

Consent for publication

All authors of this study agreed to publish.

Competing interests

The authors declare no competing interests.

Author details

[1]Department of Rheumatology, Affiliated Hospital of Nantong University, Medical School of Nantong University, Nantong 226001, China
[2]Department of Rheumatology, Renji Hospital, Shanghai Jiao Tong University School of Medicine, Shanghai 200001, China
[3]Research Center of Clinical Medicine, Affiliated Hospital of Nantong University, Medical School of Nantong University, Nantong 226001, China
[4]Department of Stomatology, Affiliated Hospital of Nantong University, Nantong 226001, China

Received: 4 March 2025 / Accepted: 1 May 2025
Published online: 16 May 2025

References

1. Parra Sanchez AR, Voskuyl AE, van Vollenhoven RF. Treat-to-target in systemic lupus erythematosus: advancing towards its implementation. Nat Rev Rheumatol. 2022;18:146–57.
2. Tsang ASMWP, Bultink IEM. New developments in systemic lupus erythematosus. Rheumatology (Oxford). 2021;60:vi21–8.
3. Yang S, Zhao M, Jia S. Macrophage: key player in the pathogenesis of autoimmune diseases. Front Immunol. 2023;14:1080310.
4. Franken L, Schiwon M, Kurts C. Macrophages: sentinels and regulators of the immune system. Cell Microbiol. 2016;18:475–87.
5. Locati M, Curtale G, Mantovani A. Diversity, mechanisms, and significance of macrophage plasticity. Annu Rev Pathol. 2020;15:123–47.
6. Funes SC, Rios M, Escobar-Vera J, Kalergis AM. Implications of macrophage polarization in autoimmunity. Immunology. 2018;154:186–95.
7. Liu Y, Luo S, Zhan Y, Wang J, Zhao R, Li Y, Zeng J, Lu Q. Increased expression of PPAR-gamma modulates monocytes into a M2-Like phenotype in SLE patients: an implicative protective mechanism and potential therapeutic strategy of systemic lupus erythematosus. Front Immunol. 2020;11:579372.
8. Li F, Yang Y, Zhu X, Huang L, Xu J. Macrophage polarization modulates development of systemic lupus erythematosus. Cell Physiol Biochem. 2015;37:1279–88.
9. Chernykh ER, Shevela EY, Starostina NM, Morozov SA, Davydova MN, Menyaeva EV, Ostanin AA. Safety and therapeutic potential of M2 macrophages in stroke treatment. Cell Transpl. 2016;25:1461–71.
10. Zhao F, Yang T, Zhou L, Zhao J, Liu J, Ping W, Zhou C, Qin Z, Jia R. Construction of tissue-engineered bladders using an artificial acellular nanocomposite scaffold loaded with stromal vascular fraction secretome. Acta Biomater. 2023;167:260–77.
11. Marar C, Starich B, Wirtz D. Extracellular vesicles in Immunomodulation and tumor progression. Nat Immunol. 2021;22:560–70.
12. Riazifar M, Mohammadi MR, Pone EJ, Yeri A, Lasser C, Segaliny AI, McIntyre LL, Shelke GV, Hutchins E, Hamamoto A, et al. Stem Cell-Derived exosomes as nanotherapeutics for autoimmune and neurodegenerative disorders. ACS Nano. 2019;13:6670–88.
13. Liu H, Tang L, Yin Y, Cao Y, Fu C, Feng J, Shen Y, Wang W. Photoresponsive multirole nanoweapon camouflaged by hybrid cell membrane vesicles for efficient antibacterial therapy of Pseudomonas aeruginosa-Infected pneumonia and wound. Adv Sci (Weinh). 2024;11:e2403101.
14. Jin Y, Xu M, Zhu H, Dong C, Ji J, Liu Y, Deng A, Gu Z. Therapeutic effects of bone marrow mesenchymal stem cells-derived exosomes on osteoarthritis. J Cell Mol Med. 2021;25:9281–94.
15. Wang Y, Liu S, Li L, Li L, Zhou X, Wan M, Lou P, Zhao M, Lv K, Yuan Y, et al. Peritoneal M2 macrophage-derived extracellular vesicles as natural multitarget nanotherapeutics to attenuate cytokine storms after severe infections. J Control Release. 2022;349:118–32.
16. Zhou M, Li YJ, Tang YC, Hao XY, Xu WJ, Xiang DX, Wu JY. Apoptotic bodies for advanced drug delivery and therapy. J Control Release. 2022;351:394–406.
17. Yu L, Zhu G, Zhang Z, Yu Y, Zeng L, Xu Z, Weng J, Xia J, Li J, Pathak JL. Apoptotic bodies: bioactive treasure left behind by the dying cells with robust diagnostic and therapeutic application potentials. J Nanobiotechnol. 2023;21:218.
18. Jiang T, Xia Y, Wang W, Zhao J, Liu W, Liu S, Shi S, Li B, He X, Jin Y. Apoptotic bodies inhibit inflammation by PDL1-PD1-mediated macrophage metabolic reprogramming. Cell Prolif. 2024;57:e13531.
19. Wen J, Creaven D, Luan X, Wang J. Comparison of immunotherapy mediated by apoptotic bodies, microvesicles and exosomes: apoptotic bodies' unique anti-inflammatory potential. J Transl Med. 2023;21:478.
20. Chen S, Zhou Y, Chen Y, Gu J. Fastp: an ultra-fast all-in-one FASTQ preprocessor. Bioinformatics. 2018;34:i884–90.
21. Butler A, Hoffman P, Smibert P, Papalexi E, Satija R. Integrating single-cell transcriptomic data across different conditions, technologies, and species. Nat Biotechnol. 2018;36:411–20.
22. Wu Y, Yang S, Ma J, Chen Z, Song G, Rao D, Cheng Y, Huang S, Liu Y, Jiang S, et al. Spatiotemporal immune landscape of colorectal Cancer liver metastasis at Single-Cell level. Cancer Discov. 2022;12:134–53.
23. Chen W, Li W, Zhang Z, Tang X, Wu S, Yao G, Li K, Wang D, Xu Y, Feng R, et al. Lipocalin-2 exacerbates lupus nephritis by promoting Th1 cell differentiation. J Am Soc Nephrol. 2020;31:2263–77.
24. Li W, Chen W, Huang S, Yao G, Tang X, Sun L. Mesenchymal stem cells prevent overwhelming inflammation and reduce infection severity via recruiting CXCR3(+) regulatory T cells. Clin Transl Immunol. 2020;9:e1181.
25. Ma Q, Liang M, Limjunyawong N, Dan Y, Xing J, Li J, Xu J, Dou C. Osteoclast-derived apoptotic bodies show extended biological effects of parental cell in promoting bone defect healing. Theranostics. 2020;10:6825–38.
26. Hu S, Chen B, Zhou J, Liu F, Mao T, Pathak JL, Watanabe N, Li J. Dental pulp stem cell-derived exosomes revitalize salivary gland epithelial cell function in NOD mice via the GPER-mediated cAMP/PKA/CREB signaling pathway. J Transl Med. 2023;21:361.

Annotation ID="1" Type="" Text="The following mandatory elements (Volume number) of the reference are missing in the Manuscript. Please check and verify." Category="Completeness" 27. Lewis SM, Williams A, Eisenbarth SC. Structure and function of the immune system in the spleen. Sci Immunol 2019, 4.

28. Chasset F, Arnaud L. Targeting interferons and their pathways in systemic lupus erythematosus. Autoimmun Rev. 2018;17:44–52.
29. Liu J, Qiu X, Lv Y, Zheng C, Dong Y, Dou G, Zhu B, Liu A, Wang W, Zhou J, et al. Apoptotic bodies derived from mesenchymal stem cells promote cutaneous wound healing via regulating the functions of macrophages. Stem Cell Res Ther. 2020;11:507.
30. Zhang Y, Shen J, Cheng W, Roy B, Zhao R, Chai T, Sheng Y, Zhang Z, Chen X, Liang W, et al. Microbiota-mediated shaping of mouse spleen structure and immune function characterized by scRNA-seq and Stereo-seq. J Genet Genomics. 2023;50:688–701.
31. Mao K, Geng W, Liao Y, Luo P, Zhong H, Ma P, Xu J, Zhang S, Tan Q, Jin Y. Identification of robust genetic signatures associated with lipopolysaccharide-induced acute lung injury onset and Astaxanthin therapeutic effects by integrative analysis of RNA sequencing data and GEO datasets. Aging. 2020;12:18716–40.
32. Constantinesco NJ, Srikanth S, De Vito L, Moras C, Ramasubramanian V, Chinnappan B, Hartwick S, Schwab KE, Wu Y, Gopal R. STAT1 regulates neutrophil gelatinase B-associated Lipocalin induction in influenza-induced myocarditis. Sci Rep. 2024;14:11124.
33. Simons KH, de Vries MR, de Jong RCM, Peters HAB, Jukema JW, Quax PHA. IRF3 and IRF7 mediate neovascularization via inflammatory cytokines. J Cell Mol Med. 2019;23:3888–96.
34. Franz S, Ertel A, Engel KM, Simon JC, Saalbach A. Overexpression of S100A9 in obesity impairs macrophage differentiation via TLR4-NFkB-signaling worsening inflammation and wound healing. Theranostics. 2022;12:1659–82.
35. Lodge M, Scheidemantle G, Adams VR, Cottam MA, Richard D, Breuer D, Thompson P, Shrestha K, Liu X, Kennedy A. Fructose regulates the Pentose phosphate pathway and induces an inflammatory and resolution phenotype in Kupffer cells. Sci Rep. 2024;14:4020.
36. Wu M, Zhou C, Li M, Yu H, Zhao D, Xue W, Qin L, Peng A. Depletion of NK cells attenuates paraquat-induced acute lung injury by manipulating macrophage polarization. Int Immunopharmacol. 2020;86:106698.
37. Frara N, Abdelmagid SM, Tytell M, Amin M, Popoff SN, Safadi FF, Barbe MF. Growth and repair factors, osteoactivin, matrix metalloproteinase and heat shock protein 72, increase with resolution of inflammation in musculotendinous tissues in a rat model of repetitive grasping. BMC Musculoskelet Disord. 2016;17:34.
38. Tukaj S, Kotlarz A, Jozwik A, Smolenska Z, Bryl E, Witkowski JM, Lipinska B. Hsp40 proteins modulate humoral and cellular immune response in rheumatoid arthritis patients. Cell Stress Chaperones. 2010;15:555–66.
39. Luo L, Wall AA, Tong SJ, Hung Y, Xiao Z, Tarique AA, Sly PD, Fantino E, Marzolo MP, Stow JL. TLR crosstalk activates LRP1 to recruit Rab8a and PI3Kgamma for suppression of inflammatory responses. Cell Rep. 2018;24:3033–44.
40. Babaeijandaghi F, Paiero A, Long R, Tung LW, Smith SP, Cheng R, Smandych J, Kajabadi N, Chang CK, Ghassemi A, et al. TNFalpha and IFNgamma cooperate for efficient pro- to anti-inflammatory transition of macrophages during muscle regeneration. Proc Natl Acad Sci U S A. 2022;119:e2209976119.
41. Dias BT, Goundry A, Vivarini AC, Costa TFR, Mottram JC, Lopes UG, Lima A. Toll-Like Receptor- and protein kinase R-Induced type I interferon sustains infection of leishmania donovani in macrophages. Front Immunol. 2022;13:801182.
42. Wang L, Yang F, Ye J, Zhang L, Jiang X. Insight into the role of IRF7 in skin and connective tissue diseases. Exp Dermatol. 2024;33:e15083.
43. Sun L, Kees T, Almeida AS, Liu B, He XY, Ng D, Han X, Spector DL, McNeish IA, Gimotty P, et al. Activating a collaborative innate-adaptive immune response to control metastasis. Cancer Cell. 2021;39:1361–e13741369.
44. Scheinecker C, Goschl L, Bonelli M. Treg cells in health and autoimmune diseases: new insights from single cell analysis. J Autoimmun. 2020;110:102376.
45. Zhang C, Li J, Cheng Y, Meng F, Song JW, Fan X, Fan H, Li J, Fu YL, Zhou MJ, et al. Single-cell RNA sequencing reveals intrahepatic and peripheral immune characteristics related to disease phases in HBV-infected patients. Gut. 2023;72:153–67.
46. Guerriero JL. Macrophages: their untold story in T cell activation and function. Int Rev Cell Mol Biol. 2019;342:73–93.
47. McGee MC, Zhang T, Magazine N, Islam R, Carossino M, Huang W. PD-1 and ICOS counter-regulate tissue resident regulatory T cell development and IL-10 production during flu. Front Immunol. 2022;13:984476.
48. Li X, Li S, Fu X, Wang Y. Apoptotic extracellular vesicles restore homeostasis of the articular microenvironment for the treatment of rheumatoid arthritis. Bioact Mater. 2024;35:564–76.
49. Pan L, Lu MP, Wang JH, Xu M, Yang SR. Immunological pathogenesis and treatment of systemic lupus erythematosus. World J Pediatr. 2020;16:19–30.
50. Zheng Y, Han Y, Sun Q, Li Z. Harnessing anti-tumor and tumor-tropism functions of macrophages via nanotechnology for tumor immunotherapy. Explor (Beijing). 2022;2:20210166.
51. Wang R, Hao M, Kou X, Sui B, Sanmillan ML, Zhang X, Liu D, Tian J, Yu W, Chen C, et al. Apoptotic vesicles ameliorate lupus and arthritis via phosphatidylserine-mediated modulation of T cell receptor signaling. Bioact Mater. 2023;25:472–84.
52. Bao P, Zheng ZT, Ye JJ, Zhang XZ. Apoptotic Body-Mediated intracellular delivery strategy for enhanced STING activation and improved tumor immunogenicity. Nano Lett. 2022;22:2217–27.
53. Zheng C, Sui B, Zhang X, Hu J, Chen J, Liu J, Wu D, Ye Q, Xiang L, Qiu X, et al. Apoptotic vesicles restore liver macrophage homeostasis to counteract type 2 diabetes. J Extracell Vesicles. 2021;10:e12109.
54. Bao L, Dou G, Tian R, Lv Y, Ding F, Liu S, Zhao R, Zhao L, Zhou J, Weng L, et al. Engineered neutrophil apoptotic bodies ameliorate myocardial infarction by promoting macrophage efferocytosis and inflammation resolution. Bioact Mater. 2022;9:183–97.
55. Zhang J, Chen C, Fu H, Yu J, Sun Y, Huang H, Tang Y, Shen N, Duan Y. MicroRNA-125a-Loaded polymeric nanoparticles alleviate systemic lupus erythematosus by restoring effector/regulatory T cells balance. ACS Nano. 2020;14:4414–29.
56. Bronte V, Pittet MJ. The spleen in local and systemic regulation of immunity. Immunity. 2013;39:806–18.
57. Sheu KM, Hoffmann A. Functional hallmarks of healthy macrophage responses: their regulatory basis and disease relevance. Annu Rev Immunol. 2022;40:295–321.
58. Chen X, Liu Y, Gao Y, Shou S, Chai Y. The roles of macrophage polarization in the host immune response to sepsis. Int Immunopharmacol. 2021;96:107791.
59. Tang L, Fu C, Liu H, Yin Y, Cao Y, Feng J, Zhang A, Wang W. Chemoimmunotherapeutic nanogel for Pre- and postsurgical treatment of malignant melanoma by reprogramming Tumor-Associated macrophages. Nano Lett. 2024;24:1717–28.
60. Burbano C, Villar-Vesga J, Vasquez G, Munoz-Vahos C, Rojas M, Castano D. Proinflammatory Differentiation of Macrophages Through Microparticles That Form Immune Complexes Leads to T- and B-Cell Activation in Systemic Autoimmune Diseases. *Front Immunol* 2019, 10:2058.
61. Horuluoglu B, Bayik D, Kayraklioglu N, Goguet E, Kaplan MJ, Klinman DM. PAM3 supports the generation of M2-like macrophages from lupus patient monocytes and improves disease outcome in murine lupus. J Autoimmun. 2019;99:24–32.
62. Sun W, Yan S, Yang C, Yang J, Wang H, Li C, Zhang L, Zhao L, Zhang J, Cheng M, et al. Mesenchymal stem cells-derived exosomes ameliorate lupus by inducing M2 macrophage polarization and regulatory T cell expansion in MRL/lpr mice. Immunol Invest. 2022;51:1785–803.
63. Qin L, Yang J, Su X, Xilan L, Lei Y, Dong L, Chen H, Chen C, Zhao C, Zhang H, et al. The miR-21-5p enriched in the apoptotic bodies of M2 macrophage-derived extracellular vesicles alleviates osteoarthritis by changing macrophage phenotype. Genes Dis. 2023;10:1114–29.
64. Shan J, Jin H, Xu Y. T cell metabolism: A new perspective on Th17/Treg cell imbalance in systemic lupus erythematosus. Front Immunol. 2020;11:1027.
65. Chavez MD, Tse HM. Targeting Mitochondrial-Derived reactive oxygen species in T Cell-Mediated autoimmune diseases. Front Immunol. 2021;12:703972.
66. Du L, Lin L, Li Q, Liu K, Huang Y, Wang X, Cao K, Chen X, Cao W, Li F, et al. IGF-2 preprograms maturing macrophages to acquire oxidative Phosphorylation-Dependent Anti-inflammatory properties. Cell Metab. 2019;29:1363–e13751368.
67. Mensali N, Grenov A, Pati NB, Dillard P, Myhre MR, Gaudernack G, Kvalheim G, Inderberg EM, Bakke O, Walchli S. Antigen-delivery through invariant chain (CD74) boosts CD8 and CD4 T cell immunity. Oncoimmunology. 2019;8:1558663.

Publisher's note